ABSTRACT

Title of thesis: A NUMERICAL STUDY OF LINK AND PATH DURATIONS IN MOBILE AD HOC NETWORKS

Hongqiang Zhang, Master of Science, 2006

Thesis directed by: Professor Richard La
Department of Electrical and Computer Engineering

A theoretical analysis has shown that under a set of assumptions, the distribution of path duration can be well approximated by an exponential distribution when the path hop count is sufficiently large. The goal of this thesis is two folds: Using NS-2 simulations to (i) Investigate how fast the path distributional convergence takes place, and how quickly the inverse of the expected duration of a path converges to the sum of the inverses of the expected durations of the links along the path, and (ii) Validate the conditions under which the distributional convergence is established.

Simulations are run under four different mobility models and two different on-demand routing protocols. Simulation results show that the path duration distribution can be accurately approximated by an exponential distribution for path hop count larger than 5 or 6 with fitting error less than 0.05 using Kolmogorov-Smirnov test (K-S test) for all considered scenarios. However, the ratio of the inverse of the expected path duration to the sum of the inverses of the expected link durations along the path does not get close to one for path hop count less than 12 in the cases

of all considered scenarios.

We validate two mixing conditions for all considered scenarios. Specifically, a sufficient condition for one mixing condition is validated. Simulation results show that the probability of one link excess life less than a positive number conditioned on the excess life of another link in the same path less than the same number behaves similarly as the CDF of the link excess life as the number decreases to 0. Based on the observation that the correlation coefficients of link excess lives decrease with increasing hop distance, instead of directly validating the second mixing condition, we validate a condition that suggests that indeed the second mixing condition is likely to hold in a large scale network. Simulation results show that the difference between the joint CDF of two link excess lives and the product of their marginal CDFs decreases as the hop distance between the two links increases.

A NUMERICAL STUDY OF LINK AND PATH DURATIONS IN MOBILE AD HOC NETWORKS

by

Hongqiang Zhang

Thesis submitted to the Faculty of the Graduate School of the
University of Maryland, College Park in partial fulfillment
of the requirements for the degree of
Master of Science
2006

Advisory Committee:

Professor Richard La, Chair/Advisor
Professor Armand Makowski
Professor Steven Tretter

DEDICATION

To my wife, my son, my parents, and my parents-in-law.

ACKNOWLEDGMENTS

I owe my gratitude to all the people who have made this thesis possible and because of whom my graduate experience has been one that I will cherish forever.

First and foremost I'd like to thank my advisor, Professor Richard La for giving me an invaluable opportunity to work on challenging and interesting projects. His guidance, patience and support throughout the research and the writing of this thesis make me unforgettable. I would also like to thank my committee members for their efforts and contributions to this work: Professor Armand Makowski and Professor Steven Tretter.

I would also like to acknowledge help and support from Seungjoon Lee and Yijie Han. Seungjoon gave me a lot of guidance on simulation at the beginning of the research that leads to the accomplishment of this thesis. The discussions with Yijie helped me a lot on the theoretical analysis. And she is always patient to answer my questions.

I owe my deepest thanks to my wife, Yang Li. Without her I would not be able to finish this work, her patience, support and encouragement are always around me. I also want to thank my parents and parents-in-law because they help me to take good care of my son, Eric during the time period when I focused on the research.

TABLE OF CONTENTS

List of Tables vi

List of Figures vii

1 Introduction 1

2 Background and Motivation 7
2.1 Related Work . . . 7
2.1.1 Basic Framework . . . 7
2.1.2 Set-up . . . 9
2.1.3 Convergence Results . . . 12
2.2 Motivation . . . 16

3 Ad Hoc Routing Protocols 18
3.1 Table-Driven Routing Protocols . . . 19
3.1.1 Destination Sequenced Distance Vector (DSDV) . . . 20
3.1.2 Wireless Routing Protocol (WRP) . . . 21
3.1.3 Cluster Switch Gateway Routing (CSGR) . . . 21
3.2 On-Demand Routing Protocols . . . 22
3.2.1 Ad Hoc On-Demand Distance Vector (AODV) . . . 23
3.2.2 Dynamic Source Routing (DSR) . . . 24
3.2.3 Temporally Ordered Routing Algorithm (TORA) . . . 25
3.2.4 Associativity-Based Routing (ABR) . . . 26
3.3 Hybrid Routing Protocols . . . 28
3.4 Comparison . . . 28

4 Mobility Models 30
4.1 Random Waypoint Model . . . 31
4.2 Manhattan Model . . . 32
4.3 Freeway Model . . . 34
4.4 Reference Point Group Mobility Model . . . 35

5 Simulation Set-up 37
5.1 Simulation Environment . . . 37
5.2 Movement Pattern . . . 39
5.3 Traffic Pattern . . . 42
5.4 Routing Protocol . . . 42
5.5 Metrics . . . 43
5.5.1 Link Duration . . . 43
5.5.2 Path Duration . . . 44
5.5.3 Link Excess Life . . . 44
5.5.4 PDF Estimation . . . 44

6 Simulation Results and Analysis 46
6.1 Link Duration and Link Excess Life PDFs 47
6.2 Path Duration CDF and Exponential Fitting 51
6.3 Relationship between the Expected Path Duration and the Expected Link Durations 57
6.4 Dependence of Link Excess Lives 60
6.5 Validation of Assumptions 62
6.5.1 Validation of the condition $D(u_n)$ 62
6.5.2 Validation of the condition $D'(u_n)$ 72
6.6 Summary and Comparison 77

7 Conclusions and Future Work 79

Bibliography 81

LIST OF TABLES

6.1 Simulation Statistics I – AODV 48

6.2 Simulation Statistics II – DSR 48

6.3 Exponential Fitting Parameter and Error I – AODV 56

6.4 Exponential Fitting Parameter and Error II – DSR 56

LIST OF FIGURES

4.1 Moving pattern of a mobile node using the Random Waypoint Mobility Model. 32

4.2 Map used in Manhattan Mobility Model. 33

4.3 Map used in Freeway Mobility Model. 34

4.4 Moving pattern of a group of 3 nodes using the RPGM Mobility Model. . 36

5.1 Flow chart of simulation. 38

6.1 PDF of link duration and link excess life for RWP 49

(a) RWP with AODV 49

(b) RWP with DSR 49

6.2 PDF of link duration and link excess life for MH 49

(a) MH with AODV 49

(b) MH with DSR 49

6.3 PDF of link duration and link excess life for FW 50

(a) FW with AODV 50

(b) FW with DSR 50

6.4 PDF of link duration and link excess life for RPGM 50

(a) RPGM with AODV 50

(b) RPGM with DSR 50

6.5 CDF of path duration and MLE exponential fitting for RWP with AODV 51

(a) 2-hop path 51

(b) 8-hop path 51

6.6 CDF of path duration and MLE exponential fitting for RWP with DSR . . 52

(a) 2-hop path 52

(b) 8-hop path . . . 52
6.7 CDF of path duration and MLE exponential fitting for MH with AODV . 52
(a) 2-hop path . . . 52
(b) 8-hop path . . . 52
6.8 CDF of path duration and MLE exponential fitting for MH with DSR . . 53
(a) 2-hop path . . . 53
(b) 8-hop path . . . 53
6.9 CDF of path duration and MLE exponential fitting for FW with AODV . 53
(a) 2-hop path . . . 53
(b) 8-hop path . . . 53
6.10 CDF of path duration and MLE exponential fitting for FW with DSR . . 54
(a) 2-hop path . . . 54
(b) 8-hop path . . . 54
6.11 CDF of path duration and MLE exponential fitting for RPGM with AODV 54
(a) 2-hop path . . . 54
(b) 8-hop path . . . 54
6.12 CDF of path duration and MLE exponential fitting for RPGM with DSR . 55
(a) 2-hop path . . . 55
(b) 8-hop path . . . 55
6.13 Ratio of inverse of average path duration to sum of inverse of average link durations along the path for RWP . . . 58
(a) RWP with AODV . . . 58
(b) RWP with DSR . . . 58
6.14 Ratio of inverse of average path duration to sum of inverse of average link durations along the path for MH . . . 58
(a) MH with AODV . . . 58

(b) MH with DSR . . . 58

6.15 Ratio of inverse of average path duration to sum of inverse of average link durations along the path for FW . . . 59

(a) FW with AODV . . . 59

(b) FW with DSR . . . 59

6.16 Ratio of inverse of average path duration to sum of inverse of average link durations along the path for RPGM . . . 59

(a) RPGM with AODV . . . 59

(b) RPGM with DSR . . . 59

6.17 Correlation coefficient as a function of hop distance for RWP . . . 60

(a) RWP with AODV . . . 60

(b) RWP with DSR . . . 60

6.18 Correlation coefficient as a function of hop distance for MH . . . 61

(a) MH with AODV . . . 61

(b) MH with DSR . . . 61

6.19 Correlation coefficient as a function of hop distance for FW . . . 61

(a) FW with AODV . . . 61

(b) FW with DSR . . . 61

6.20 Correlation coefficient as a function of hop distance for RPGM . . . 62

(a) RPGM with AODV . . . 62

(b) RPGM with DSR . . . 62

6.21 Plot of $\left|\mathbf{P}\left[X_i \leq x_1, X_{i+k} \leq x_2\right] - \mathbf{P}\left[X_i \leq x_1\right]\ \mathbf{P}\left[X_{i+k} \leq x_2\right]\right|$ where $k = 1, 3, 5, 7$ for RWP with AODV . . . 64

6.22 Plot of $\left|\mathbf{P}\left[X_i \leq x_1, X_{i+k} \leq x_2\right] - \mathbf{P}\left[X_i \leq x_1\right]\ \mathbf{P}\left[X_{i+k} \leq x_2\right]\right|$ where $k = 1, 3, 5, 7$ for RWP with DSR . . . 65

6.23 Plot of $\left|\mathbf{P}\left[X_i \leq x_1, X_{i+k} \leq x_2\right] - \mathbf{P}\left[X_i \leq x_1\right]\ \mathbf{P}\left[X_{i+k} \leq x_2\right]\right|$ where $k = 1, 3, 5, 7$ for MH with AODV . . . 66

6.24 Plot of $\left|\mathbf{P}\left[X_i \leq x_1, X_{i+k} \leq x_2\right] - \mathbf{P}\left[X_i \leq x_1\right] \mathbf{P}\left[X_{i+k} \leq x_2\right]\right|$ where $k = 1, 3, 5, 7$ for MH with DSR 67

6.25 Plot of $\left|\mathbf{P}\left[X_i \leq x_1, X_{i+k} \leq x_2\right] - \mathbf{P}\left[X_i \leq x_1\right] \mathbf{P}\left[X_{i+k} \leq x_2\right]\right|$ where $k = 1, 3, 5, 7$ for FW with AODV 68

6.26 Plot of $\left|\mathbf{P}\left[X_i \leq x_1, X_{i+k} \leq x_2\right] - \mathbf{P}\left[X_i \leq x_1\right] \mathbf{P}\left[X_{i+k} \leq x_2\right]\right|$ where $k = 1, 3, 5, 7$ for FW with DSR 69

6.27 Plot of $\left|\mathbf{P}\left[X_i \leq x_1, X_{i+k} \leq x_2\right] - \mathbf{P}\left[X_i \leq x_1\right] \mathbf{P}\left[X_{i+k} \leq x_2\right]\right|$ where $k = 1, 3, 5, 7$ for RPGM with AODV 70

6.28 Plot of $\left|\mathbf{P}\left[X_i \leq x_1, X_{i+k} \leq x_2\right] - \mathbf{P}\left[X_i \leq x_1\right] \mathbf{P}\left[X_{i+k} \leq x_2\right]\right|$ where $k = 1, 3, 5, 7$ for RPGM with DSR 71

6.29 Plot of the CDF and the conditional probabilities for RWP with AODV . 73

(a) $\mathbf{P}\left[X_{\ell+1} \leq c | X_\ell \leq c\right]$ 73

(b) $\mathbf{P}\left[X_{\ell+k} \leq c | X_\ell \leq c\right]$, $k = 2, 4$ 73

6.30 Plot of the CDF and the conditional probabilities for RWP with DSR . . . 74

(a) $\mathbf{P}\left[X_{\ell+1} \leq c | X_\ell \leq c\right]$ 74

(b) $\mathbf{P}\left[X_{\ell+k} \leq c | X_\ell \leq c\right]$, $k = 2, 4$ 74

6.31 Plot of the CDF and the conditional probabilities for MH with AODV . . 74

(a) $\mathbf{P}\left[X_{\ell+1} \leq c | X_\ell \leq c\right]$ 74

(b) $\mathbf{P}\left[X_{\ell+k} \leq c | X_\ell \leq c\right]$, $k = 2, 4$ 74

6.32 Plot of the CDF and the conditional probabilities for MH with DSR . . . 75

(a) $\mathbf{P}\left[X_{\ell+1} \leq c | X_\ell \leq c\right]$ 75

(b) $\mathbf{P}\left[X_{\ell+k} \leq c | X_\ell \leq c\right]$, $k = 2, 4$ 75

6.33 Plot of the CDF and the conditional probabilities for FW with AODV . . 75

(a) $\mathbf{P}\left[X_{\ell+1} \leq c | X_\ell \leq c\right]$ 75

(b) $\mathbf{P}\left[X_{\ell+k} \leq c | X_\ell \leq c\right]$, $k = 2, 4$ 75

6.34 Plot of the CDF and the conditional probabilities for FW with DSR . . . 76

(a) $\mathbf{P}\left[X_{\ell+1} \leq c | X_\ell \leq c\right]$ 76

(b) $\mathbf{P}\left[X_{\ell+k} \leq c | X_\ell \leq c\right]$, $k = 2, 4$ 76

6.35 Plot of the CDF and the conditional probabilities for RPGM with AODV 76

(a) $\mathbf{P}\left[X_{\ell+1} \leq c | X_\ell \leq c\right]$ 76

(b) $\mathbf{P}\left[X_{\ell+k} \leq c | X_\ell \leq c\right]$, $k = 2, 4$ 76

6.36 Plot of the CDF and the conditional probabilities for RPGM with DSR . . 77

(a) $\mathbf{P}\left[X_{\ell+1} \leq c | X_\ell \leq c\right]$ 77

(b) $\mathbf{P}\left[X_{\ell+k} \leq c | X_\ell \leq c\right]$, $k = 2, 4$ 77

Chapter 1

Introduction

Multi-hop wireless ad hoc networks have been an active research area in recent years. In mobile ad hoc networks, nodes can be connected dynamically in an arbitrary manner. There is no stationary infrastructure of the network. Each node behaves as a router and participate in discovery and maintenance of routes to other nodes in the network. Ad hoc networks have many applications. For example, a rescue team communicate with each other in a disaster recovery scene using mobile devices. Another example is that a military group coordinate in a battlefield where there is no existing communication network available.

In general, a multi-hop wireless ad hoc network can be viewed as a collection of mobile nodes with communication and networking capability. These nodes can establish and maintain a network without intervention or an infrastructure. As nodes move around, they establish and tear down links between them. This implies that the connectivity between nodes in the network changes more frequently and dynamically than in a wired network. As a result, network topology varies with time. The routing protocols designed for wired networks (*e.g.,* the Internet) generally use either *distance vector* or *link state* routing algorithms. In distance vector routing, each router periodically broadcasts to its neighbor routers its view of the distance to all hosts. In link state routing, each router instead periodically broadcasts to all

other routers in the network its view of the status of its adjacent network links. Due to the frequent changes of link status and network topology, these routing protocols will incur high overhead to update and maintain the route information between any pair of nodes in a mobile ad hoc network (MANET). Therefore, the routing protocols used in wired networks are rather inefficient if used in MANETs.

Over the past years, many new routing protocols have been proposed for MANETs to handle such frequent network topology changes [2], [3], [4], [5], [6]. Routing protocols for wireless ad hoc networks are largely classified as being either table-driven (proactive) or on-demand (reactive). In table-driven protocols, the routing table at each node is periodically exchanged and updated. Each node maintains the route information to all known destinations at all times. In on-demand protocols, a route discovery procedure is triggered only when there is no path available to use between a source and a destination. Moreover, nodes are not required to maintain the route to every known destination in the network.

When one or more of the links along a path break down (called a path failure), the data packets that uses the failed path cannot be delivered until an alternative path is established through a route discovery procedure. Hence, a path failure will not only disrupt the ongoing services associated with the data packets, but also incur additional overheads. Thus, a good routing protocol should attempt to select a path with longer duration to reduce the frequency of path failures when more than one path are discovered.

The performance of a routing protocol is likely to be shaped by the statistical properties of link and path durations. Intuitively, a path duration is closely

determined by the link durations along the path and their dependence structure. Therefore, the statistical properties of link and path durations and their relation are of interest. In particular, understanding the characteristics of link and path durations can help not only network engineers to design better routing protocols that provide reliable services at reduced overhead, but also better evaluate the performance of on-demand routing protocols, without running time-consuming detailed simulations.

In [37], Sadagopan *et al.* first presented a simulation study of the multi-hop path duration distributions under four mobility models. Their simulation results show that the path duration distribution can be accurately approximated by an exponential distribution when the path hop count is larger than 3 or 4 for all mobility models considered. However, there is no explanation offered for the emergence of an exponential distribution, and the relation between link and path durations was not studied. Besides, it is not mentioned in the paper if the minimum speed of nodes is larger than 0 which is critical for Random Waypoint (RWP) mobility model. In RWP model, the average speed of nodes decreases to 0 over time if the minimum speed of nodes is set to 0 [29]. Such speed decay can have a dramatic influence on time-averaged metrics. For example, average link duration obtained over an earlier time period may be quite different from that obtained over a later time period.

Han *et al.* [18] developed an approximate framework for studying the distribution properties of link and path durations. They assume that the link excess lives are mutually independent. The link excess life is defined as the interval of time from the moment a path is established to the moment one of its links breaks

down. Then by applying Palms Theorem [21, Thm. 5-14, p. 157], they showed that, under a certain set of conditions, the path duration distribution converges to an exponential distribution under appropriate scaling when the path hop count is sufficiently large. This result is consistent with the simulation results provided in [37]. In addition, they also explored the relation between the expected path duration and the expected link durations. The analysis revealed that the inverse of the expected path duration is approximately given by the sum of the inverses of the expected link durations along the path. However, it is generally not true that the link excess lives are mutually independent. For instance, consider two adjacent links along a path. Since they have a common node, the common node's mobility affects the excess lives of both links. This suggests that the link excess lives are dependent. Although the simulation results showed the correlation between the excess lives of the links is weak in the case of RWP model, this may not be the case for other mobility models.

In [20], Han *et al.* relaxed the independence assumption on the reachability processes imposed in [18]. Instead, they assume that the dependence of link excess lives goes away asymptotically as the hop distance between the links in a path increases. This assumption is stated using a mixing condition. A second mixing condition is also introduced for establishing the similar distributional convergence of path duration with dependent link excess lives. They demonstrated that under a set of mild conditions, the same distributional convergence to an exponential distribution shown in [18] holds. Furthermore, they showed that the same relation between the expected path duration and the expected link durations in [18] still

holds. This means that the parameter of emerging exponential distribution does not depend on the dependence of the link excess lives under the given conditions. Simulations were run in a relatively large scale network with 200 nodes and a strictly positive minimum speed of nodes under RWP and Manhattan (MH) mobility models. However, they did not validate two mixing conditions, and no simulation study was carried out for the relation between the expected path duration and the expected link durations along the path.

In this thesis, we carry out simulation studies of the link and path duration distributions and their relation in a multi-hop wireless ad hoc network using network simulator (NS-2 [24]). We run extensive simulations under a total of eight different scenarios by using four different mobility models and two different on-demand routing protocols. Our goal is two folds: (1) Investigate how fast the distributional convergence occurs, and how quickly the inverse of the expected duration of a path converges to the sum of the inverses of the expected durations of the links along the path, and (2) Validate the conditions in [20] under which the path distributional convergence is established.

The rest of thesis is organized as follows. Chapter 2 describes the previous related work on the link and path duration distributions and the motivation for our work. Chapter 3 presents an overview of a set of routing protocols proposed for MANETs. Chapter 4 gives an overview of four different mobility models proposed for MANETs and used in our simulations. Chapter 5 describes the simulation settings in detail. In particular, it explains (1) how we generate nodes movement and traffic connections in the network with selected parameters, (2) how we record the links

and paths information through the routing protocols during the simulations, and (3) how we compute the distributions of link and path durations, link excess life, etc. In Chapter 6, detailed simulation results are provided for eight scenarios. We give the simulation numbers, plot the distributions of link and path durations as well as link excess life. We perform exponential fitting and compute the fitting errors between the empirical distributions and the fitting curves of path duration distributions. We also compute the correlation coefficients of the link excess lives for studying the dependence level of link excess lives as a function of hop distance between the links, and validate two mixing conditions. Finally, Chapter 7 concludes with a discussion on future work that may help to further understand the link and path duration distributions.

Chapter 2

Background and Motivation

In this chapter, we first describe the related work in [18] and [20]. Then,we state the motivation of our work.

2.1 Related Work

In this section, we summarize the results reported in [18] and [20]. Section 2.1.1 describes a model for studying the path duration. It describes the setup and teardown of a link and a path. It also gives the definition of link duration, path duration, link excess life and their corresponding mathematical expressions. Section 2.1.2 introduces a parametric scenario used to study the statistical properties of path durations with large path hop counts. Section 2.1.3 presents the distributional convergence of path duration with increasing path hop count.We use the same notation as in [20].

2.1.1 Basic Framework

We consider a MANET with N nodes. These nodes move across a domain $\mathbb{D}$ of $\mathbb{R}^2$ or $\mathbb{R}^3$ according to some mobility model [20]. An on-demand routing protocol is assumed to be used.

Since nodes can move in an unpredictable manner, links between nodes are

set up and torn down dynamically. A link is established between two nodes once they become aware of each other. For example, a link is established between two nodes when the two nodes move within the transmission range of each other, or when the signal-to-interference-noise-ratio (SINR) at the receiving node exceeds certain threshold, and packets can be reliably decoded at the receiving node. A *link duration* is defined to be the amount of time that passes from the moment the link is established to the moment the link breaks down. Communication links are assumed bidirectional to ensure reliable communication between two nodes.

If there is a sequence of links available at the same time connecting a source and a destination, a path can be established from the source to the destination. A *path duration* is the amount of time that elapses from the moment a path is established until the moment one of the links along the path breaks down. For simplicity, path setup delays are assumed negligible. A *link excess life or time-to-live* is the amount of time that elapses from path setup time to the moment one or more of its link break down.

Now, we describe the model for studying the path duration. We define a time-varying graph with nodes as vertices and available links as edges of the graph: Let $V = \{1, \ldots, N\}$ denote the set of N nodes. For two distinct nodes i and j in V, a $\{0,1\}$-valued *reachability* process $\{\xi_{ij}(t),\ t \geq 0\}$ is used to describe a link status – "up" or "down". When $\xi_{ij}(t) = 1$ (resp. $\xi_{ij}(t) = 0$), the link between nodes i and j is up (resp. down) at time $t \geq 0$. And, $\xi_{ij}(t) = \xi_{ji}(t)$ holds because links are assumed bidirectional. The process $\{\xi_{ij}(t),\ t \geq 0\}$ is an alternating on-off process. The successive up and down time durations are described

by two sequences of rvs $\{U_{ij}(k), k = 1, 2, \ldots\}$ and $\{D_{ij}(k), k = 1, 2, \ldots\}$, respectively [20]. There are many ways to define the reachability process. One example (used in this analysis) is that two nodes can communicate with ('or 'reach") each other if they are within some fixed transmission range. Let $r_{min} > 0$ be some fixed transmission range and $\boldsymbol{X}_i(t)$ denote the position of node i at time $t \geq 0$. Then $\xi_{ij}(t) := \mathbf{1}\left[||\boldsymbol{X}_i(t) - \boldsymbol{X}_j(t)|| \leq r_{min}\right], \quad t \geq 0$ (known as protocol model [16], [32]).

A time-varying graph $(V, E(t))$ is defined with $E(t) := \{(i, j) \in V \times V : \xi_{ij}(t) = 1\}, \quad t \geq 0$ where by convention, $\xi_{ii}(t) = 0$ for each i in V and all $t \geq 0$. If node d is reachable from node s by a set of edges in the *undirected* graph derived from the directed graph $(V, E(t))$, a path can be established between nodes s and d at time $t \geq 0$. Let $\mathcal{P}_{sd}(t)$ denote the set of paths from node s to node d. When non-empty, there may be more than one path in the set $\mathcal{P}_{sd}(t)$ [20]. Then the routing protocol selects one of them. Let $\mathcal{L}_{sd}(t)$ denote the set of links in the selected path.

For each link $\ell \in \mathcal{L}_{sd}(t)$, let $T_\ell(t)$ denote the time-to-live (or excess life) of link ℓ after time t. Let $Z_{sd}(t)$ denote the duration of the established path from node s to node d using the links in $\mathcal{L}_{sd}(t)$. Based on the definition of path duration stated earlier in this section, the path duration can be written as [20]

$$Z_{sd}(t) := \min\left(T_\ell(t) : \ell \in \mathcal{L}_{sd}(t)\right), \quad t \geq 0 \tag{2.1}$$

2.1.2 Set-up

Because we are interested in studying the path duration distribution with large path hop counts, we introduce the following parametric scenario. For each

$n = 1, 2, \ldots$, let $V^{(n)} = \{1, \ldots, N^{(n)}\}$ and $\mathbb{D}^{(n)}$ denote the set of mobile nodes and the domain across which the nodes move, respectively. A superscript (n) is used to denote the dependence on n.

Before we present the path duration in this model, the following assumptions are introduced.

1. The stochastic process that governs the arrival of path requests is assumed to be independent of the nodes trajectory processes.

2. Scaling – The situation of interest is the one where $N^{(n)} \sim nN^{(1)}$ and Area($\mathbb{D}^{(n)}$) $\sim n \cdot$Area($\mathbb{D}^{(1)}$) as $n \to \infty$. It is customary to reparameterize so that $N^{(n)} = n$, *i.e.,* n is the total number of nodes in a network.

3. Stationarity – As the system is expected to run for a long time, we can assume that steady state has been reached. This can be modeled by taking the $\frac{N^{(n)} \times (N^{(n)}-1)}{2}$ reachability processes $\{\xi_{ij}^{(n)}(t),\ t \geq 0\}$ to be *jointly stationary.* For distinct nodes $i < j$ in $V^{(n)}$, let the sequence of rvs $\{(U_{ij}^{(n)}(k), D_{ij}^{(n)}(k)),\ k = 2, 3, \ldots\}$ denote the sequence of up and down times for the reachability process $\{\xi_{ij}^{(n)}(t),\ t \geq 0\}$, the sequence $\{(U_{ij}^{(n)}(k),\ D_{ij}^{(n)}(k)),\ k = 2, 3, \ldots\}$ is required to be a stationary sequence. Let $(U_{ij}^{(n)},\ D_{ij}^{(n)})$ denote the generic marginals of the sequence $\{(U_{ij}^{(n)}(k),\ D_{ij}^{(n)}(k)),\ k = 2, 3, \ldots\}$, and let $G_{ij}^{(n)}$ denote the cumulative distribution function (CDF) of $U_{ij}^{(n)}$, *i.e.,* $G_{ij}^{(n)}$ is the CDF of duration of link (i, j) [20].

Under such a setup, well-known results for renewal processes [21, Sections 5-6] can be generalized as follows: With $\ell = (i, j)$ and the notation introduced in Section

2.1.1, $P[T_\ell^{(n)}(0) \le x \Big| \xi_{ij}^{(n)}(0) = 1] = F_\ell^{(n)}(x), \quad x \in \mathbb{R}$ [1], where $F_\ell^{(n)}$ is given by

$$F_\ell^{(n)}(x) = \begin{cases} \frac{1}{m(G_\ell^{(n)})} \int_0^x (1 - G_\ell^{(n)}(y))\, dy\ , & \text{if } x > 0 \\ 0\ , & \text{if } x \le 0 \end{cases} \tag{2.2}$$

for some link duration CDF $G_\ell^{(n)}$. Equation (2.2) gives the relation between the distribution of link duration and link excess life. The distribution $F_\ell^{(n)}$ is simply the forward recurrence time distribution associated with $U_\ell^{(n)}$. From (2.2) it is easy to see that link excess life has a non-increasing probability density function (PDF). This will be numerically validated in Chapter 6.

The set $\mathcal{L}_{sd}^{(n)}(0)$ of links is a random subset of $E(0)$. It is assumed that a pair of nodes s and d in $V^{(n)}$ can be selected such that $\lim_{n\to\infty} |\mathcal{L}_{sd}^{(n)}(0)| = \infty$. For convenience, the sequence $\{|\mathcal{L}_{sd}^{(n)}(0)|, n = 1, 2, \ldots\}$ is assumed to be deterministic.

Let $X_\ell^{(n)}$ denote any $\mathbb{R}_+$-valued rv $X_\ell^{(n)} =_{st} \left[T_\ell^{(n)}(0) \le x \Big| \xi_{ij}^{(n)}(0) = 1\right]$ [2], *i.e.,* $X_\ell^{(n)}$ is used to denote a link excess life. Then, the distribution of $X_\ell^{(n)}$ is given by $F_\ell^{(n)}$. The path duration $Z_{sd}(t)$ in (2.1) can now be viewed as the path duration $Z^{(n)}$ (between nodes s and d, we remove subscript (sd) without causing any confusion) defined by

$$Z^{(n)} := \min\{X_\ell^{(n)} :\ \ell = 1, \ldots, H(n)\} \tag{2.3}$$

where $H(n) = |\mathcal{L}_{sd}^{(n)}(0)|$ is the path hop count with $\lim_{n\to\infty} H(n) = \infty$.

[1] Due to the stationarity assumptions, it suffices to consider only the case $t = 0$.

[2] Two rvs X and Y with the same distribution are denoted by $X =_{st} Y$.

2.1.3 Convergence Results

Having described the model for studying the path duration, we present the results of path duration distribution under two situations in the next two subsections.

A. Independent Link Excess Lives

In [18], Han *et al.* assume that the reachability processes $\{\xi_{ij}^{(n)}(t),\ t \geq 0\}$ are mutually independent, and so are the link excess lives $\{X_\ell^{(n)},\ \ell = 1, \ldots, H(n)\}$. They introduce the following assumptions.

Assumption 1 (scaling) *There exists* $\lambda > 0$ *such that*

$$\lim_{n\to\infty} \frac{1}{H(n)} \sum_{\ell=1}^{H(n)} \lambda_\ell^{(n)} = \lambda$$

where $\lambda_\ell^{(n)} = \left(m(G_\ell^{(n)})\right)^{-1}$, $\ell = 1, \ldots, H(n),\ n = 1, 2, \ldots$.

Assumption 2 *For every* $x \geq 0$,

$$\lim_{n\to\infty} \left(\max_{\ell=1,\ldots,H(n)} G_\ell^{(n)}(\frac{x}{H(n)}) \right) = 0\ .$$

Assumption 2 can be restated as follows: For each $x \geq 0$ and an arbitrarily small $\varepsilon > 0$, there exists an integer $n^\star = n^\star(x;\varepsilon)$ such that

$$\max_{\ell=1,\ldots,H(n)} G_\ell^{(n)}(\frac{x}{H(n)}) \leq \varepsilon, \quad for\ n\ \geq\ n^\star$$

Theorem 1 *Under Assumptions 1-2, the following holds*

$$\lim_{n\to\infty} \mathbf{P}\left[H(n) \cdot Z^{(n)} \leq x\right] = \begin{cases} 1 - e^{-\lambda x} & \text{if } x > 0 \\ 0 & \text{if } x \leq 0 \end{cases} . \tag{2.4}$$

Theorem 1 states that when the number of hops along the path is large enough, the path duration distribution can be accurately approximated by an exponential distribution under Assumptions 1-2. Furthermore, it also suggests that the inverse of the mean path duration is approximately given by the sum of the inverses of the mean link durations along the path, *i.e.,* $(\mathbf{E}[Z^{(n)}])^{-1} \simeq \sum_{l=1}^{H(n)} (m(G_l^{(n)}))^{-1}$, when path hop count is large enough.

In general, however, the reachability processes $\{\xi_{ij}^{(n)}(t),\ t \geq 0\}$ $(i < j$ in $V^{(n)})$ are not mutually independent, and the link excess lives $X_\ell^{(n)}$, $\ell = 1, \ldots, H(n)$ are not independent either. This is discussed in the following subsections.

B. Dependent Link Excess Lives

In a more general case that Han *et al.* considered in [20], they only assume that the dependence of link excess lives goes away asymptotically with increasing hop distance between links. The hop distance is defined as the number of hops between two links. For example, hop distance one means there is only one hop between two links, *i.e.,* neighboring links. This assumption is stated using a *mixing condition*. Also, a second mixing condition is introduced for establishing a similar distributional convergence of path duration with dependent link excess lives.

Let $\boldsymbol{W} := \{W_i^{(n)}, n = 1, 2, \ldots; i = 1, 2, \ldots, h(n)\}$ be an array of $\mathbb{R}$-valued rvs, where $\{h(n), n \geq 1\}$ is a set of positive integers with $\lim_{n\to\infty} h(n) = \infty$ and $\{u_n, n = 1, 2, \ldots\}$ be a sequence of (positive) real numbers. Denote the joint CDFs of rvs $\{W_{i_1}^{(n)}, \ldots, W_{i_n}^{(n)}\}$ by $\mathbf{J}_{i_1 \cdots i_n}(\cdot)$. For notational brevity, we write $\mathbf{J}_{i_1 \cdots i_n}(u)$ for $\mathbf{J}_{i_1 \cdots i_n}(u, \ldots, u)$.

In order to prove the distributional convergence, the following two mixing conditions are introduced in [20].

Definition 1 *($D(u_n)$ condition [22], [23]) The array* $\mathbf{W}$ *is said to satisfy the condition $D(u_n)$ if for any integers*

$$1 < i_1 < \cdots < i_p < j_1 < \cdots < j_q \leq h(n) \quad with \quad j_1 - i_p > m$$

we have

$$\left| \mathbf{J}^{(n)}_{i_1 \ldots i_p j_1 \ldots j_q}(u_n) - \mathbf{J}^{(n)}_{i_1 \ldots i_p}(u_n) \mathbf{J}^{(n)}_{j_1 \ldots j_q}(u_n) \right| \leq \alpha_{n,m} \ , \tag{2.5}$$

where $\lim\limits_{n\to\infty} \alpha_{n,m(n)} = 0$ *for some sequence* $\{m(n), n = 1, 2, \ldots\}$ *that satisfies (i)* $\lim_{n\to\infty} m(n) = \infty$ *and (ii)* $m(n) = o(h(n))$*, i.e.,* $\lim_{n\to\infty} \frac{m(n)}{h(n)} = 0$.

The condition $D(u_n)$ imposes a form of "dependency decay" as the distance $(j_1 - i_p)$ of two sets of rvs $\{W^{(n)}_{i_1}, \ldots, W^{(n)}_{i_p}\}$ and $\{W^{(n)}_{j_1}, \ldots, W^{(n)}_{j_q}\}$ increases. In Section 6.5.1, instead of directly validating the condition $D(u_n)$, we validate a condition that suggests that indeed the condition $D(u_n)$ is likely to hold in a large scale network.

Any finite set E of consecutive positive integers $\{j_1, \ldots, j_2\}$ is referred as an "interval" with length $j_2 - j_1 + 1$. Let k be a fixed positive integer, and $\{m(n), n = 1, 2, \ldots\}$ denote a sequence of positive integers such that $k < m(n) < n' = \lfloor h(n)/k \rfloor$ [3] for all sufficiently large n.

[3] $\lfloor h(n)/k \rfloor$ denotes the integer part of $h(n)/k$.

Definition 2 *The array* $\mathbf{W}$ *is said to satisfy the condition* $D'(u_n)$ *if*

$$\lim_{n\to\infty}\Big(\sum_{i,i'\in I_{k,j}^{(n)}:i<i'}\mathbf{P}\left[W_i^{(n)}>u_n,W_{i'}^{(n)}>u_n\right]\Big)=o\left(\frac{1}{k}\right)\quad \textit{for all } j=1,\ldots,k\ . \tag{2.6}$$

where $I_{k,j}^{(n)}=\{(j-1)\cdot n'+1,\ldots,j\cdot n'\}$ for $j=1,\ldots,k$.

A sufficient condition for condition $D'(u_n)$ to hold is that

$$\lim_{n\to\infty}\left\lfloor\frac{H(n)}{k}\right\rfloor^2\cdot\sup_{i,i'\in I_{k,j}^{(n)}:i<i'}\mathbf{P}\left[W_i^{(n)}>u_n,W_{i'}^{(n)}>u_n\right]=o\left(\frac{1}{k}\right) \tag{2.7}$$

for all $j=1,\ldots,k$. We validate a sufficient condition for (2.7) in Section 6.5.2.

The following assumptions are introduced to prove the distributional convergence.

Assumption 3 *For any sequence of intervals* $\hat{I}^{(n)}\subset\{1,\ldots,H(n)\}$, $n\geq 1$,

$$\frac{1}{H(n)}\sum_{i\in\hat{I}^{(n)}}\lambda_l^{(n)}=O\left(\frac{|\hat{I}^{(n)}|}{H(n)}\right)\ .$$

A *sufficient* condition for Assumption 3 is that there exists some arbitrarily small positive constant ε such that $\mathbf{m}(G_\ell^{(n)})\geq\varepsilon$ for all $n=1,2,\ldots$ and $\ell=1,\ldots,H(n)$.

Assumption 4 *Let* $\boldsymbol{W}:=\{(X_\ell^{(n)})^{-1},n=1,2,\ldots;\ell=1,,\ldots,H(n)\}$. *The array* $\boldsymbol{W}$ *satisfies the mixing conditions* $D(u_n)$ *and* $D'(u_n)$ *with sequence* $u_n=\frac{H(n)}{x}$ *for any* $x\in(0,\infty)$.

If we take the sequence $u_n=H(n)/x$, then the condition $D'(u_n)$ implies that rare events $\{X_i^{(n)}<\frac{x}{H(n)}\}$ are not strongly correlated in its neighborhood as $n\to\infty$ (hence $H(n)\to\infty$).

Theorem 2 *Suppose that Assumptions 1 - 4 hold. Then, we have*

$$\lim_{n\to\infty} \mathbf{P}\left[H(n)\cdot Z^{(n)} \leq x\right] \;=\; \begin{cases} 1-e^{-\lambda x}\,, & \text{if } x>0 \\ 0\,, & \text{if } x\leq 0 \end{cases}. \tag{2.8}$$

Theorem 2 states that the same path distribution convergence to an exponential distribution shown in (2.4) holds. This suggests that the distributional convergence does not depend on the dependence of link excess lives under the given assumptions. It also tells us that the expected duration of a path is approximately given by $\mathbf{E}[Z^{(n)}] \simeq \frac{1}{\sum_{\ell=1}^{H(n)}(m(G_\ell^{(n)}))^{-1}}$ for sufficiently large path hop count. This implies that the parameter of the emerging exponential distribution is not affected by the dependence of link excess lives under the given assumptions.

2.2 Motivation

The results presented in [37], [18], and [20] suggest that the path duration distribution can be well approximated by an exponential distribution under a set of conditions when the path hop count is sufficiently large. The work in [18] and [20] also reveals the relation between the expected path duration and the expected link durations along a path.

The goal of this thesis is two folds: (1) Investigate how fast the distributional convergence occurs, and how quickly the inverse of the expected duration of a path converges to the sum of the inverses of the expected durations of the links along the path, and (2) Validate the conditions $D(u_n)$ and $D'(u_n)$ introduced in [20] under which the path distributional convergence is established.

The finding on the convergence of an expected path duration can be used to provide a guidance for a new path selection scheme proposed in [20]. In that scheme, an expected path duration is estimated using the sum of the inverses of the estimated expected durations of the links along the path. Therefore, this finding can tell when such an estimate is accurate.

Chapter 3

Ad Hoc Routing Protocols

An ad hoc wireless network has unique characteristics or limitations. First, mobile nodes in an ad hoc network are allowed to move in an uncontrolled or unpredictable manner. This implies frequent and unpredictable link and path set-ups and tear-downs between the nodes in the network. Routing protocols must accommodate such dynamic changes. Second, the underlying wireless channel provides much lower and more variable bandwidth than a wired network. The sharing of wireless channel reduces the available bandwidth to each node. Thus, routing protocols should be bandwidth efficient by introducing a minimal amount of routing overhead. Third, since many of mobile nodes are expected to run on batteries, it is desirable to have an energy efficient routing protocol as well. This also demands low overhead.

Routing protocols developed for wired networks require routers to periodically broadcast routing information between each other. Due to the frequent changes of link status and network topology, these routing protocols will incur high overhead to update and maintain the route information between any pair of nodes in MANET. Therefore, the routing protocols used in wired networks are rather inefficient if used in MANETs. Since the 1970s, many routing protocols have been developed for mobile ad hoc networks [2] [3] [4] [5] [6] [10]. These protocols are generally

categorized as table-driven (proactive), on-demand (reactive) and hybrid. Table-driven routing protocols attempt to maintain a path between any two nodes at all times, whereas on-demand routing protocols establish a path between two nodes only upon request.

The rest of this chapter is organized as follows: Section 3.1 provides an overview of available table-driven routing protocols in ad hoc wireless networks. Section 3.2 gives an overview of available on-demand routing protocols. Section 3.3 describes hybrid routing protocols. Section 3.4 makes a simple comparison between table-driven and on-demand routing protocols.

3.1 Table-Driven Routing Protocols

Table-driven routing protocols attempt to maintain consistent, up-to-date routing information for every pair of nodes. Each node maintains one or more routing tables to store routing information. When a change of network connectivity occurs, this information will propagate throughout the network to keep the consistency of routing information at each node. The protocols differ in the number of routing tables and the methods of route update propagation. Table-driven protocols incur low overhead and performs well when routing information updates take place infrequently. However, when network topology changes frequently, they lead to large overhead and poor performance.

3.1.1 Destination Sequenced Distance Vector (DSDV)

The DSDV routing protocol is based on the idea of the classical distributed Bellman-Ford routing algorithm with certain improvement [4]. Each mobile node maintains a routing table that lists all available destinations, the hop count to reach each of them and the sequence number assigned by the destination node. The sequence number is used to distinguish stale routes from new ones and thus avoid the formation of routing loops. The newer route has higher sequence number. A path with minimal hop count is chosen when there are more than one path with same sequence number available. Each node periodically sends its routing table to its immediate neighbors. When a significant change has occurred in a node's table since the last update, it also sends its routing table to its adjacent neighbors. Therefore the update is both time-driven and event-driven.

There are two ways to update a routing table: a "full dump" or an "incremental update". A full dump means the full routing table is sent to the neighbors and could span many packets. An incremental update only involves those entries in the routing table that have changed since the last update, and the update information must fit into one packet. Therefore, when the network is relatively stable, incremental updates are used to avoid extra traffic and full dumps are relatively infrequent. In a fast-changing network, incremental packets can grow large and full dump will be more frequent, rendering an inefficient utilization of network resources.

3.1.2 Wireless Routing Protocol (WRP)

In WRP protocol [7] [8], nodes send the distance and second-to-last hop information for each destination in the network. Each node is forced to verify the consistency of second-to-last hop information reported by all its neighbors to overcome the *count-to-infinity* problem and provide faster route convergence. Each node must maintain four tables: (a) distance table, (b) routing table, (c) link-cost table, and (d) message retransmission list (MRL) table. The distance table contains the hop count between a node and its destination. The routing table contains the next hop node. The link-cost table reflects the delay associated with a particular link. The MRL table records which updates in an update message need to be retransmitted and which neighbors should acknowledge the retransmission. Each node maintains its neighbors list by either receiving a HELLO message or packets from them. Update messages are periodically sent to nodes' neighbors to ensure the accurate up-to-date routing information. A path with minimum delay (shortest-path) will be used.

3.1.3 Cluster Switch Gateway Routing (CSGR)

The CSGR protocol uses DSDV as the underlying routing scheme. However, it adopts a hierarchical cluster-head-to-gateway routing approach to route traffic from a source to a destination [9]: Mobile nodes are grouped into clusters and each cluster has a cluster head which is responsible for relaying the traffic within the cluster through the gateway. Gateway nodes are nodes that are within the

transmission range of two or more cluster heads. Each node maintains two tables: cluster member table and routing table. A cluster member table stores the cluster head information of the destinations and is updated periodically using the DSDV protocol. A routing table contains the next hop to the destination. On receiving a packet, a node will check its cluster member table to find out the nearest cluster head and then look up its routing table to get the next hop node to reach that cluster head. The packet is first routed to a gateway, and then to another cluster head. This repeats until the packet reaches the cluster head of the destination. The packet is then routed to the destination at the end.

3.2 On-Demand Routing Protocols

On-demand routing protocols establish a path between a source and a destination only when desired by the source node. A path discovery procedure is triggered when there is no valid path available between the source and the destination in the routing table at the source. A route maintenance procedure is used to deal with the link status changes. Unlike table-driven protocols, nodes do not need to maintain the up-to-date routing information for each destination at all times. This kind of protocols are desirable when the network topology changes frequently; the overhead increases only with the arrival rate of route requests and the additional control overhead due to topology change.

3.2.1 Ad Hoc On-Demand Distance Vector (AODV)

The AODV protocol is built on the DSDV algorithm. It uses a sequence number and a route table to prevent routing loops and maintain route information.

There are two phases in the AODV protocol: route discovery and route maintenance. A route discovery procedure is initiated by a source broadcasting a route request (RREQ) message to its neighbors. Once an intermediate node with a valid route or the destination node receives the RREQ message, it unicasts a route reply (RREP) message to its neighbor from which it first received the RREQ message. If an intermediate node does not have a route to the destination , it forwards the RREQ message to its neighbors. This repeats until the RREQ message reaches the destination node or an intermediate node with a valid route. A broadcast ID, source node IP address and its sequence number are used to uniquely identify an RREQ packet. During the process of forwarding the RREQ, intermediate nodes record in their route tables the address of neighbors from which the first copy of the broadcast packet was received, thereby establishing a reverse path. Additional copies of the same RREQ are discarded silently. The first discovered route is selected by the source node. Each node only needs to know the next hop to the destination but not the full hop-by-hop path. As the RREP is routed back along the reverse path, nodes along this path set up forward route entries in their route tables that point to the node from which the RREP came. These forward route entries indicate the active forward route. Each route entry also has a timer to reflect the freshness of the route entry.

Nodes broadcast a HELLO message periodically to maintain local connectivity information. When there is a link failure along a route due to a node's movement, if the break point is close to the destination node, the upstream node of the broken link will perform a local repair by initiating a route discovery and forward the new RREP to the source node through its upstream nodes along the route. If not, this node propagates a route error (RERR) message to each of its active upstream neighbors. These nodes in turn propagate the RERR message to their upstream neighbors until the source node is reached. The source node may initiate another route discovery if desired.

3.2.2 Dynamic Source Routing (DSR)

The DSR protocol is based on the concept of source routing [3]. Unlike the AODV protocol, the source knows the complete hop-by-hop route to the destination. Thereby it is guaranteed to be loop-free. The route information is stored in a route cache and data packets carry the source route in the packet header. Entries in the route cache are continually updated as new routes are learned.

Similar to AODV, DSR consists of two phases: route discovery and route maintenance. When a node has packets to send, it will first look up its route cache to determine if there is a route ready for use. If it has one valid route to the destination, it will go ahead and use this route. Otherwise, it will broadcast a RREQ packet. Each node receiving a RREQ packet checks if it has a route to the destination. If not, it adds its own address into the route record of the packet

and rebroadcasts it to its neighbors only when the request has not yet been seen before and the node's own address does not already appear in the route record. A RREP packet is generated when either the destination receives the RREQ packet or an intermediate node with a valid route in its route cache receives the packet. In both cases, the route record will be updated to contain the full path information and put into the RREP packet. Then the RREP packet is sent back to the source via either the reverse path or a path in the route cache. In contrast to AODV, DSR uses route cache to store complete route information, and there are multiple routes available in the route cache for each source destination pair. A path with minimum hop count is selected when several paths are available.

Route maintenance is accomplished through the use of RERR packets and acknowledgments. When a link is detected broken, a RERR packet is broadcast, all nodes that receive the packet will update their route caches by deleting the hop in error and truncating the routes that contain the hop at that point.

3.2.3 Temporally Ordered Routing Algorithm (TORA)

The TORA protocol is a highly adaptive, loop-free, distributed routing algorithm based on the concept of link reversal. It is proposed to operate in a highly dynamic mobile networking environment [6]. It provides multiple routes for any source destination pair. The key feature of TORA is that the control messages are localized to a very small set of nodes near the occurrence of a topological change.

The TORA protocol performs three basic functions: route creation, route

maintenance and route erasure. During the route creation and route maintenance, nodes use a "height" metric to establish a directed acyclic graph (DAG) rooted at the destination. Each link is assigned a direction (upstream or downstream) based on the relative height metric of two end nodes. A downstream link is established from a node with a higher reference level to a node with a lower reference level.

When there is a link failure, nodes generate a new reference level accordingly and propagates to their neighbors so that all involved nodes change their reference levels accordingly. Links are reversed to reflect the change and a new DAG is reestablished rooted at the destination. Timing is an important factor for TORA because the "height" metric is dependent on the temporal order of the topological changes. Therefore, in order to implement TORA in a real ad hoc network, all nodes require to be synchronized by accessing to an external time source such as the Global Positioning System (GPS). Route erasure essentially involves flooding a "clear packet" throughout the network to erase invalid routes.

3.2.4 Associativity-Based Routing (ABR)

The ABR protocol attempts to provide a path that is likely to be more stable than other available paths by introducing a new metric in path selection step during the route discovery and route reconstruction phase. This new metric is called associativity which is a measure of the level of spatial, temporal, and connection stability of a link [38] [39]. Each node constantly monitors the beacons transmitted from its neighbors and records the number of beacons it receives. This number is

called its associativity with a particular neighbor. The higher value of the number means less mobility of the node , while the low value of the number indicates high mobility of the node. Hence the path should be established using stable links (high associativity) for long path duration. Each node maintains a separate associativity for each of its neighbors.

When a source needs to establish a route, it broadcasts a query message. Each intermediate node puts its address into the packet header and rebroadcasts the query until it reaches the destination. The associativities with its neighbors are also be appended to the packet header. However, an intermediate node will erase its upstream neighbor's associativities and keep only those concerned with itself and its upstream neighbor. When a destination receives a broadcast query from multiple paths, it chooses the path that has the maximum average associativity (*i.e.,* the aggregated associativity divided by the hop count) and uses the hop count to break a tie. The destination then sends a reply packet along the selected path to the source. The other discovered routes are then deleted.

When a link on a route breaks down due to node mobility, local reconstruction of the route is attempted first before the source rebroadcasts another route query. The upstream node of the broken link broadcasts a query to discover an alternative route. The destination also performs the path selection when receives this query.

3.3 Hybrid Routing Protocols

A hybrid protocol combines the merits of table-driven and on-demand routing protocols. An example is Zone Routing Protocol (ZRP) [10]. Each node specifies a quantity called zone radius measured in number of hops. A node's routing zone is defined as a collection of nodes whose minimum hop distance from the node in question is less than its zone radius. The ZRP protocol uses a table-driven routing algorithm for intra-zone communication and an on-demand routing algorithm for inter-zone communication. Each zone has some border nodes for intra-zone communication. This kind of protocols are attractive due to lower overhead compared with purely table-driven routing protocols. However, because a route may involve different independent routing protocols for different parts of the route, it might be very difficult to assure the route stability.

There are also other types of routing protocols such as signal stability routing (SSR) protocol, location-aware routing (LAR) protocol and power-aware routing (PAR) protocol [11] [12].

3.4 Comparison

Table-driven routing protocols require each nodes to maintain the up-to-date routing information for any other nodes in the network. In order to accomplish it, routing information update must be broadcast in the network whenever there is a topology change. It is apparent that when the network topology changes rapidly the system will use most bandwidth and power to perform the routing information

update even though some routing information may not be used. Therefore the network performance will be poor. On the other hand, on-demand routing protocols initiate a path discovery process only upon request. The routing overhead scales with the arrival rate of the source requests. It may introduce a delay when there is no route available for a packet delivery. But the overall performance will be better than the table-driven routing protocols when the source requests rate is lower than the frequency of network topology changes. In [13], Johansson *et al.* compared the performance of three routing protocols under three simulation scenarios with different nodes speed range. The results showed that AODV and DSR have much better performance than DSDV in terms of packet delivery ratio, throughput and overhead under the scenarios with the rapid movement of the nodes. In this thesis, we use AODV and DSR in our simulations.

Chapter 4

Mobility Models

In MANETs, mobility models play an important role on the performance of routing protocols [26]. A mobility model is designed to describe the movement pattern of mobile nodes such as how their speeds and positions update over time. A mobility model should attempt to mimic the real movements of real mobile nodes. Currently there are two ways to generate the mobility models: trace method and synthetic method. The trace method uses the real life mobile nodes' traces to get accurate movement information. However, it is not easy to get real traces due to the lack of deployment of ad hoc mobile networks. Hence, synthetic method is used in most of current research.

There are different ways to categorize the synthetic mobility models. Camp *et al.* in [26] separate the mobility models into entity models and group models. The entity models simulate the movement of independent mobile nodes in the network, *i.e.,* there is no correlation between the movement of any two mobile nodes. The group models on the other hand simulate the movement of nodes which is correlated with the movement of other nodes. In [35], various mobility models are categorized into several classes in terms of their specific mobility characteristics such as total randomness, spatial dependency, temporal dependency and geographic restriction.

In this chapter, we describe four different mobility models proposed in the past

and also used in our simulations: Random Waypoint (RWP) model, Manhattan (MH) model, Freeway (FW) model and Reference Point Group Mobility (RPGM) model.

4.1 Random Waypoint Model

The RWP model is widely used in the MANET research community due to its simple implementation and analysis [1] [27] [28]. In this model, each node is assigned an initial position uniformly distributed within a region. Then, each node chooses a destination uniformly inside the region, and selects a speed uniformly from [*minspeed*, *maxspeed*] independently of the chosen destination. The node then moves toward the chosen destination with the selected speed along a straight line starting from current waypoint. After reaching the destination, the node stops for a duration called "pause time", and then repeats the procedure. All nodes move independently of each other at all times. Fig. 4.1 shows an example of moving pattern of a mobile node using the RWP model starting at a randomly chosen position (20, 1230).

It has been shown that the average speed of nodes at steady-state in the RWP model is $\bar{S} = \frac{S_{max}-S_{min}}{ln(S_{max})-ln(S_{min})}$ [29], where S_{min} and S_{max} are the minimum and maximum speed of nodes, respectively. The steady-state means that the distributions of nodes' speeds and locations are stationary. It is easily seen from the above equation that $\bar{S}$ decreases over time to zero if $S_{min} = 0$. A simple solution to overcome such speed decay is to assign a positive S_{min}.

It is generally true that the distributions of nodes' speeds and locations vary

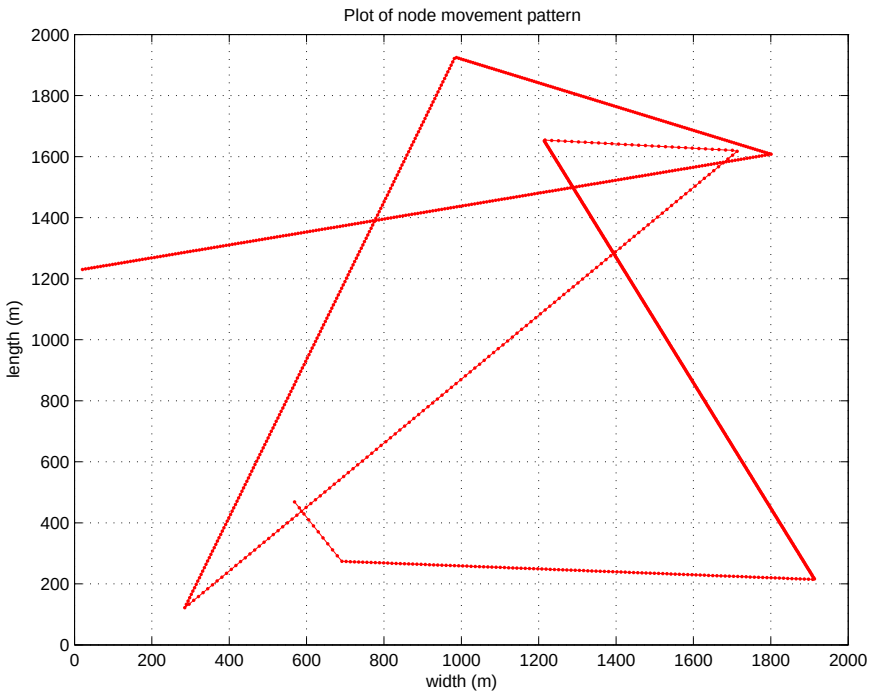

Figure 4.1: Moving pattern of a mobile node using the Random Waypoint Mobility Model.

continuously over time and converge to a steady-state distribution. The issue here is how to deal with such transient period. One solution is to choose the nodes' initial locations and speeds according to the stationary distribution [27] [30] to avoid the transient period from the beginning. Another one is to discard the initial time period of simulation to reduce the effect of such transient period on simulation results.

4.2 Manhattan Model

The MH model is used to emulate the nodes movement on streets defined by maps [36]. An example map is shown in Fig. 4.2. The application of the MH model is modeling movement in an urban area where a pervasive computing service between portable devices is provided.

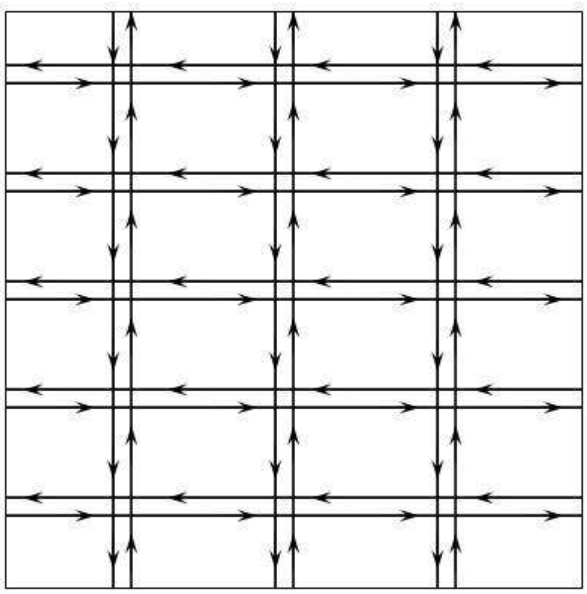

Figure 4.2: Map used in Manhattan Mobility Model.

The map is composed of a number of horizontal and vertical streets. Each street has two lanes, one in each direction (North and South for vertical streets, and East and West for horizontal ones). Each node is only allowed to move along the grid of horizontal and vertical streets. At an intersection of horizontal and vertical streets, a mobile node can turn left, or right, or go straight with probabilities 0.25, 0.25, and 0.5, respectively. The speed of a mobile node is temporarily dependent on its previous speed. The speed of a node $s(t)$ is updated according to: $s(t+1) = \min(S_{max}, \max(0, s(t) + a(t) \cdot X))$ where $X \sim Uniform[-1, 1]$, and $a(t)$ is Acceleration Speed.

4.3 Freeway Model

The FW model is similar to the MH model in that it also needs a predefined map [36]. But the map here can contain horizontal, vertical and diagonal freeways. Fig. 4.3 shows an example map with only one freeway. This model can be useful in tracking a vehicle on a freeway.

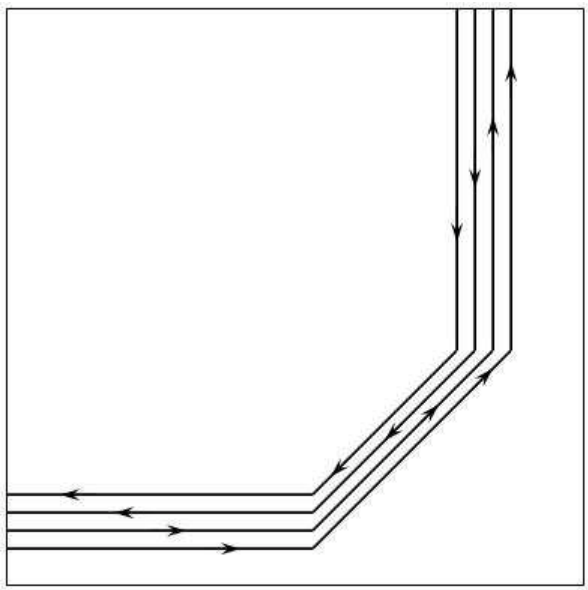

Figure 4.3: Map used in Freeway Mobility Model.

Each freeway has lanes in both directions (left to right and right to left, bottom to top and top to bottom, bottom left to upper right and upper right to bottom left). A node is restricted to its lane on the freeway. The speed of a node is temporally dependent on its previous speed. And, the nodes on the same lane follow the rule that the speed of a node cannot exceed the speed of the node ahead of it when they

are within the Safety Distance (SD). The relationships can be written as:

a) $s(t+1) = \min(S_{max}, \max(0, s(t) + a(t) \cdot X))$, *where* $X \sim Uniform[-1, 1]$ *and* $a(t)$ *is Acceleration Speed*;

b) *for any distinct nodes* i *and* j, *and* $t \geq 0$, $D_{ij}(t) \leq SD \Rightarrow s_i(t) \leq s_j(t)$ *if* j *is ahead of* i *in the same lane, where* $D_{ij}(t)$ *is the distance between nodes* i *and* j *at time* t.

4.4 Reference Point Group Mobility Model

The RPGM model may contain one or more logical groups. Each group has a logical leader that determines the group's motion behavior [34] [36]. The difference between the RPGM model and the above three models is that nodes' movements are not totally independent but are dependent within a group. The RPGM model can be applied in military battlefield communications where the commander and soldiers form a logical group, or in a disaster recovery area where a rescue team and a medical team form logical groups.

Initially, each member of a group is uniformly distributed in the neighborhood of the group leader. At each time instant, each member is assigned a reference point which follows the group leader's movement. Then each member is randomly placed in the neighborhood of its reference point. Members always move within some fixed maximum distance from the group leader. Thus, a group trajectory is determined by the path of the leader. Fig. 4.4 shows one example of the movement pattern of a group containing 3 nodes.

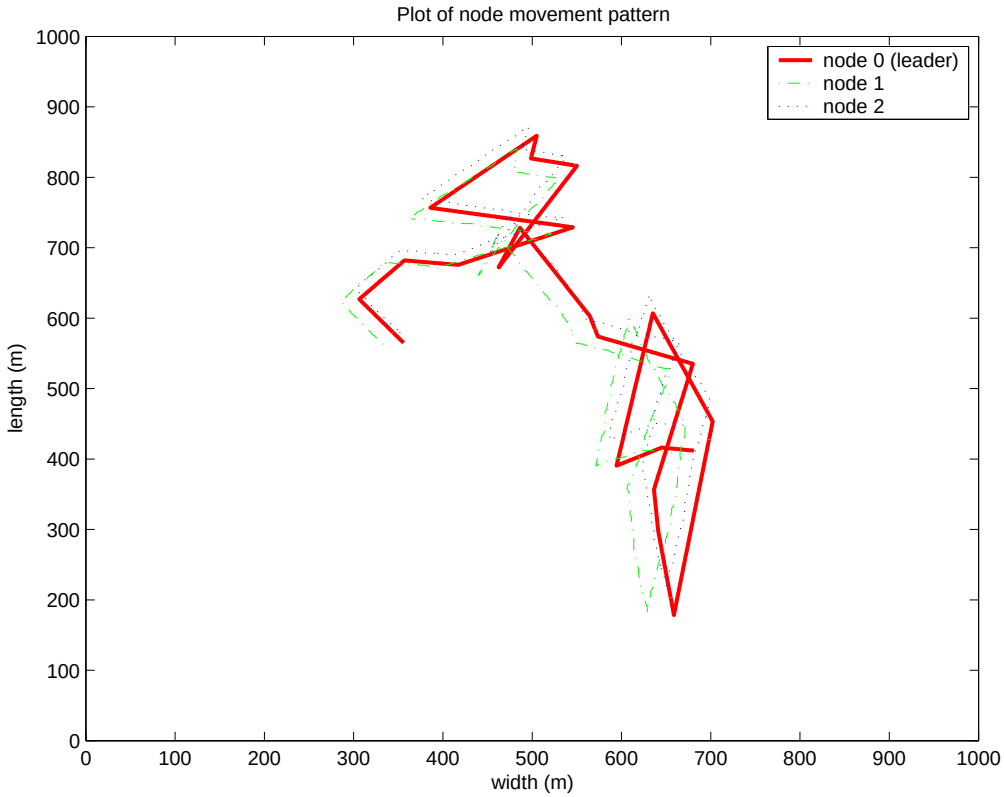

Figure 4.4: Moving pattern of a group of 3 nodes using the RPGM Mobility Model.

Chapter 5

Simulation Set-up

In order to get the link and path duration distributions, we need to (1) generate different movement patterns and traffic pattern for the simulation program, (2) extract nodes movement information and path setup information during the simulation, and (3) compute the link duration, link excess life and path duration. Moreover, we use the above information to compute other quantities of interest, *e.g.,* correlation coefficients of link excess lives, and to validate the conditions that are introduced in [18] [20]. All simulations are carried out using network simulator 2 (NS-2) on a PC (Pentium 4, 3.0 GHz, 1 GB RAM) running Fedora Core 3. Fig. 5.1 shows a flow chart of simulation. In the rest of this chapter, we will describe simulation setup in detail.

5.1 Simulation Environment

NS-2 is a discrete time event-driven network simulator developed at UC Berkeley and is now a part of Virtual InterNetwork Testbed (VINT) project [24]. It simulates various IP networks, including network protocols such as TCP (Transmission Control Protocol) and UDP (User Datagram Protocol), traffic source behavior such as CBR (Constant Bit Rate), router queue management mechanism such as Drop Tail, RED (Random Early Detection), etc.

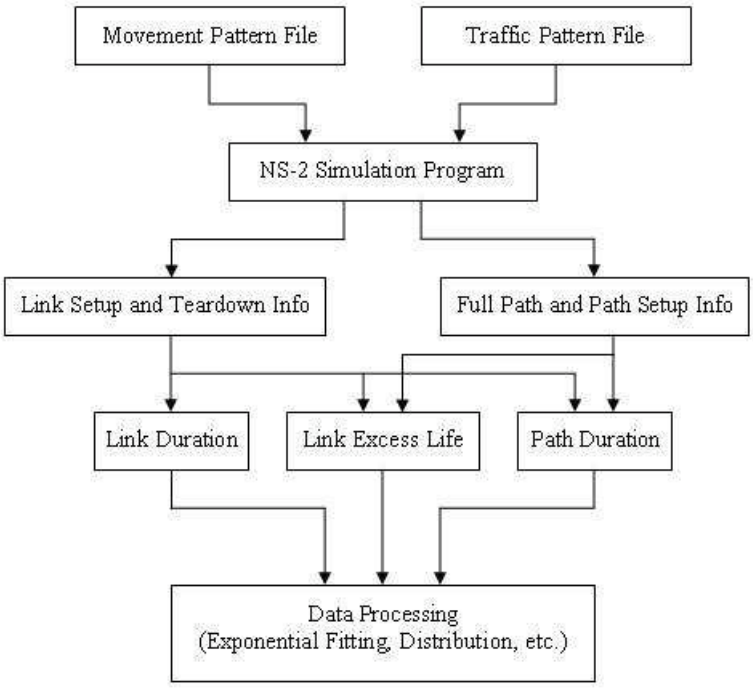

Figure 5.1: Flow chart of simulation.

In a recent paper [28], the Monarch research group at Carnegie Mellon University developed support for simulating multi-hop wireless networks complete with physical, data link, and medium access control (MAC) layer models on existing NS-2. The radio propagation model includes Friis free space model, two ray ground reflection model at far distance or shadowing model. Each mobile node has an interface queue maintained as a priority queue to hold the packets awaiting for transmission. The Distributed Coordination Function (DCF) of IEEE 802.11 for wireless LANs is used as the MAC layer protocol [25]. An unslotted carrier sense multiple access scheme with collision avoidance (CSMA/CA) is used to transmit data packets.

NS-2 is an open source project and is continually evolving. In this thesis, we use the version ns-2.28.

5.2 Movement Pattern

We use four mobility models − RWP, MH, FW, and RPGM to generate movement patterns. For the RWP model, NS-2 has a program called "*setdest*" to generate such a movement pattern with flexible model parameters. [1] For the MH and FW models, we use the programs developed for IMPORTANT project at USC [36]. For the RPGM model, we use the package tool called "BonnMotion" developed at University of Bonn. However, we modify the programs of MH and FW to handle the boundary hitting situations: In MH, when a mobile node hits the boundary of the domain, it makes a U-turn and moves in the opposite direction on the same street (but on the opposite lane). Similarly, in FW, when a mobile node hits the boundary, it makes a U-turn and moves in the opposite direction on the same freeway (but on an opposite lane chosen uniformly from available lanes).

For all four models, the simulations are run on a rectangular region of 2 km × 2 km. There are 200 nodes moving across this region, and the transmission range of these nodes is fixed at 200 m. For RWP, MH, and FW models, the speed range of nodes is [0.2, 6] m/s. For RPGM model, the speed of a node is chosen from [1, 10] m/s. The specific parameters associated with each model are listed below. Each simulation period lasts for 1200 seconds. However, we discard the first 400 seconds and only consider the last 800 seconds. In this way, we try to reduce the effect of transient period on simulation results.

[1] In version ns-2.28, *setdest* already implements selecting the nodes' speeds according to the stationary distribution of speeds [30] [27] at the beginning of simulation.

- **RWP**

  Initially, all nodes are uniformly distributed in the rectangular region. Then, all nodes move continually according to the model without stop, *i.e.,* the pause time is 0. Based on the equation (2) in [29], the average speed of nodes at steady state in this case is equal to 1.71 m/s.

- **MH**

  There are a total of 32 streets - 19 horizontal streets and 13 vertical streets in the rectangular region. Each street has two lanes, one in each direction (North and South for vertical streets and East and West for horizontal streets). The horizontal streets are separated by 100 m, and the vertical ones are separated by 150 m. The distance between two neighboring lanes in opposite directions on the same street is 5 m. The speed of a mobile node $s(t)$ is updated every 1 second according to $s(t+1) = \min(6; \max(0; s(t) + 0.6 \cdot X))$ m/s, where $X \sim$ Uniform[-1, 1]. At the beginning of the simulation, all nodes are uniformly distributed on the streets, and the speeds of all nodes are uniformly distributed between 0.2 and 6 m/s. Then, the nodes move along the lanes and update their speeds and directions accordingly.

- **FW**

  There is only one freeway with a total of 6 lanes in the rectangular region. Each lane contains 3 segments (horizontal, diagonal and vertical) and has a direction as shown in Fig. 4.3. The distance between two neighboring lanes of a freeway is 5 m. The first (horizontal) segment of the bottom lane starts

from the left boundary of the region with length 1200 m, and is 50 m away from the bottom boundary of the region. The second (diagonal) segment has angle 45° from the horizontal line. The third (vertical) segment is 50 m away from the right boundary of the region. The speed of a mobile node $s(t)$ is updated every 1 second according to $s(t+1) = \min(6; \max(0; s(t) + 0.6 \cdot X))$ m/s, where $X \sim$ Uniform[-1, 1]. If node j and node i are in the same lane and node j is ahead of node i, when they are within the safety distance (SD) 40 m, $s_i(t) \leq s_j(t)$. Initially, all nodes are uniformly distributed on the freeway (or lanes), and the speeds of the nodes are uniformly distributed in [0.2, 6] m/s. Each node moves along the lanes and updates its speed and direction accordingly.

- **RPGM**

  First, 10 nodes are randomly chosen from all nodes and form one group. Then, another 10 nodes are randomly chosen from the rest after the 1st selection and form another group. This process repeats until each node is in one group. Therefore, there is a total of 20 groups with 10 in each one. Each node is marked with a distinct non-negative integer. The node with minimal number in a group is the leader in that group. The maximum distance between the leader and a group member is set to 100 m. Initially each group member is uniformly distributed around the group leader inside a circle of radius 100 m, and the node speed is uniformly distributed in [1, 10] m/s. All nodes move without pause throughout the entire simulation period.

5.3 Traffic Pattern

Here, the traffic pattern means how data packets arrive at the nodes in the network. We use CBR traffic source. However, a source sends only one packet to a destination. The reason is that sending one data packet is sufficient for a routing protocol to discover a path from the source to the destination and record the path setup information. We can use such information to compute the path duration and link excess life offline with the link setup information. The source-destination pairs are randomly chosen from all nodes. The packet interarrival time follows an exponential distribution with average value 6 seconds. For the purpose of simplifying extracting paths information, a large average interarrival time (6 seconds) is used. The packet size is 64 bytes. The first traffic connection starts at $t = 400\ s$ since we discard the data from first 400 seconds. Because one simulation period is only 1200 seconds which cannot hold enough number of traffic connections, each simulation run consists of more than one simulation period. For each simulation period, a different movement pattern and a different traffic pattern are used. For each scenario considered, we generate more than 30,000 connections.

5.4 Routing Protocol

We run simulations using AODV and DSR routing protocols. But, we modify both protocols implemented in NS-2 to print out the path information during the simulation which is used for computing the path durations, link excess lives, etc. In AODV, when a destination receives the RREQ packet, it sends a RREP

packet back to the source along the reverse path discovered during the route discovery process. As an intermediate node along the path receives the RREP packet, it extracts the node that sends the packet to it and prints out the node number as well as its own node number in the format "$LINK \quad Node_{send} \quad Node_{recv}$". When the RREP packet reaches the source, the source first print outs the link information in the same format as above. Then, the source extracts the destination from the packet and prints out the path information with the path setup time in the format "$SRCDST \quad Node_{src} \quad Node_{dst} \quad at \quad T_{path-setup}$". From the printout, we extract the hop-by-hop path information.

In DSR, when the source receives an RREP packet from either an intermediate node or a destination, it extracts the complete hop-by-hop path information from the packet, saves in its route cache, and prints out the path information with the path setup time in the format "$SRCDST - RR \quad [hop - by - hop - path] \quad at \quad T_{path-setup}$".

5.5 Metrics

For the purpose of measuring the link and path durations, the transmission range of the mobile nodes is set to 200 m. It can be changed by varying the receiver power threshold. Any two nodes separated by a distance less than or equal to the transmission range has a communication link between them.

5.5.1 Link Duration

During the simulation period, we log the nodes' movement information every 1 second in an output trace file. After the simulation, we extract the movement information from the trace file, and thus get a snapshot of the network connectivity every 1

second. Hence, we know exactly the link status between any pair of nodes throughout the entire simulation period with time resolution of 1 second. Link durations are calculated offline. The output format of the link status information from the calculation is "$Node_i - Node_j \quad T_{link-setup} \quad T_{link-breakdown}$".

5.5.2 Path Duration

As described in Section 5.4, the hop-by-hop path information and its setup time is recorded during the simulation. Once we know the path setup time and the link status information, the path duration can be computed as follows: First, for each link along the path we compute the time at which the link goes down for the first time after path setup. Then, we find the link that goes down first. The time interval between the path setup time and the link teardown time gives the path duration. The output format of the path information is "$[hop-by-hop-path] \quad hop-count \quad T_{path-setup} \quad Path_{Duration}$".

5.5.3 Link Excess Life

The link excess life defined before can be computed in a straightforward manner once the path setup time and the link status information is known.

5.5.4 PDF Estimation

After simulations, we use the relative frequency approach (from standard probability theory) to calculate the empirical PDFs of link and path durations as well as that of link excess life for each scenario. After computing the PDFs, we compute (i) the empirical CDFs of link and path durations as well as that of link excess life, and (ii) the empirical joint CDFs of link excess lives. For path durations, we calculate a separate CDF for each

path hop count. The detailed simulation results and analysis are provided in next chapter.

Chapter 6

Simulation Results and Analysis

In this chapter, we present the details of the simulation results from different scenarios. We run the simulations under eight different scenarios, each using one of four mobility models and one of two routing protocols. Using collected data,

1. We plot the distributions of link duration and link excess life, and validate the PDF of link excess life is non-increasing as implied by (2.2) (or (9) in [20]).

2. We find that the path duration distribution can be well approximated by an exponential distribution with fitting error less than 0.05 using KS-test when the path length is at least 6 or 7 hops for all scenarios. In addition, in the case of MH model, the path duration distribution matches the exponential fitting curve well with fitting error less than 0.05 even when the path length is as small as 2 hops.

3. We show that even for path hop count greater than 10, the parameter obtained from exponential fitting is not very close to the sum of the inverses of the expected link durations along a path. This suggests slow convergence of the parameter. The maximum path hop count is limited to 12 hops due to limited domain size.

4. We study the level of local dependence in link excess lives by computing the correlation coefficients of link excess lives under different scenarios. Simulation results show weak dependence as hop distance between links increases. For RWP, MH, and FW models, the dependence is fairly weak for non-neighboring links. For RPGM model, the dependence is non-negligible if the hop distance is less than 5.

5. We validate two mixing conditions defined in (2.5) and (2.6) (or in (14) and (16) in [20]). Specifically, we validate a sufficient condition for the condition $D'(u_n)$. Based on the simulation results of the level of dependence in link excess lives, rather than validate the condition $D(u_n)$ directly, we validate a condition that suggests that indeed the condition $D(u_n)$ is likely to hold in a large scale network.

6.1 Link Duration and Link Excess Life PDFs

As stated in the previous chapter, we record the setup and breakdown times of all links, hop-by-hop paths and their setup times during each simulation run. Then, we compute empirical distributions of link duration, link excess life, and path duration. The numbers of links and paths statistics collected for all eight scenarios are listed in Table 6.1 (with AODV) and 6.2 (with DSR). Here we only consider the links that are used to provide a path during the simulation. Also, we only consider path hop counts with more than 1,000 samples.

Table 6.1: Simulation Statistics I – AODV

	RWP with AODV	MH with AODV	FW with AODV	RPGM with AODV
# of links	260,906	233,214	173,000	135,502
# of 1-hop paths	1,621	1,495	3,624	8,170
# of 2-hop paths	2,859	1,841	2,593	4,254
# of 3-hop paths	3,727	2,203	2,542	4,945
# of 4-hop paths	4,325	2,535	2,522	3,691
# of 5-hop paths	4,833	2,844	2,265	3,108
# of 6-hop paths	4,767	3,126	2,221	2,492
# of 7-hop paths	4,824	3,377	2,047	1,937
# of 8-hop paths	4,165	3,279	1,949	1,304
# of 9-hop paths	3,579	3,044	1,687	1,062
# of 10-hop paths	2,913	2,693	1,526	-
# of 11-hop paths	2,234	2,163	1,467	-
# of 12-hop paths	1,568	1,754	1,277	-

Table 6.2: Simulation Statistics II – DSR

	RWP with DSR	MH with DSR	FW with DSR	RPGM with DSR
# of links	235,217	205,212	16,346	126,957
# of 1-hop paths	1,085	1,005	1,391	4,167
# of 2-hop paths	1,847	1,100	2,338	4,350
# of 3-hop paths	2,666	1,364	2,210	3,830
# of 4-hop paths	3,291	1,626	2,332	3,822
# of 5-hop paths	3,673	2,026	2,384	3,106
# of 6-hop paths	4,034	2,293	2,368	2,742
# of 7-hop paths	4,281	2,628	2,273	2,276
# of 8-hop paths	3,840	2,802	2,270	1,862
# of 9-hop paths	3,452	2,963	2,145	1,220
# of 10-hop paths	2,926	2,557	2,018	-
# of 11-hop paths	2,248	1,937	1,874	-
# of 12-hop paths	1,722	1,543	1,762	-

The empirical distributions of link duration and link excess life are plotted in Figs. 6.1 – 6.4. From the plots, we note that the PDF of link excess life is non-increasing under all scenarios. This follows directly from (8) in [18] (or in (2.2)).

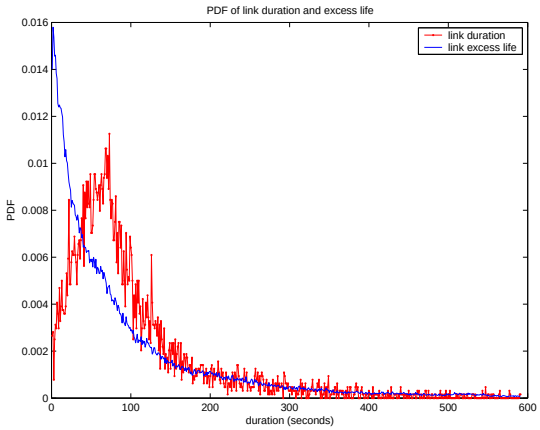

(a) RWP with AODV

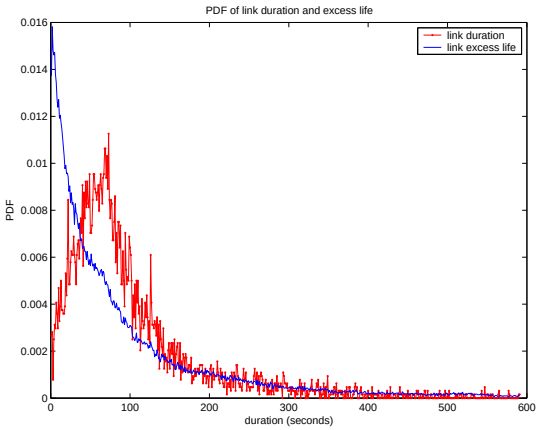

(b) RWP with DSR

Figure 6.1: PDF of link duration and link excess life for RWP

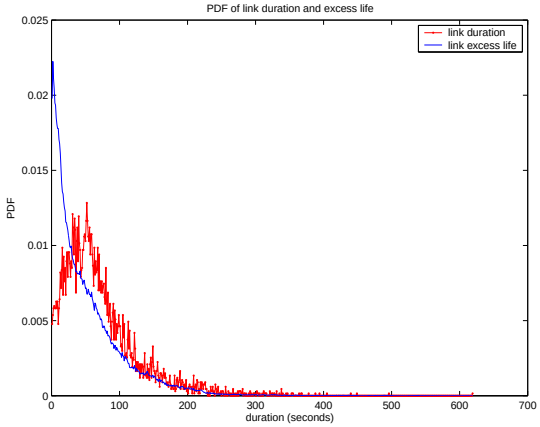

(a) MH with AODV

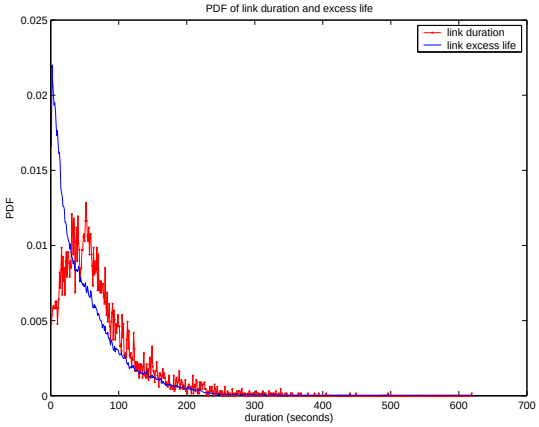

(b) MH with DSR

Figure 6.2: PDF of link duration and link excess life for MH

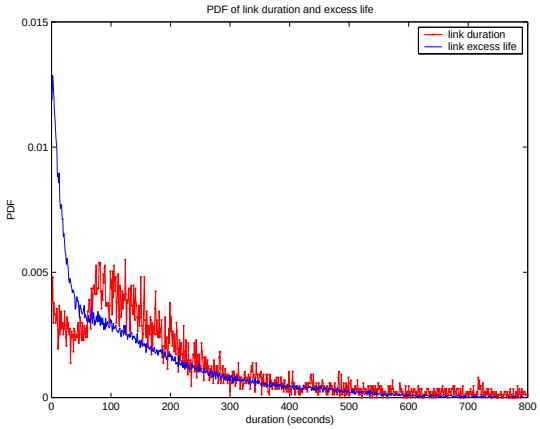

(a) FW with AODV

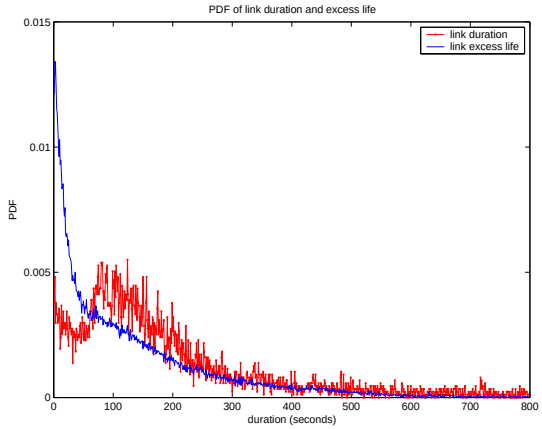

(b) FW with DSR

Figure 6.3: PDF of link duration and link excess life for FW

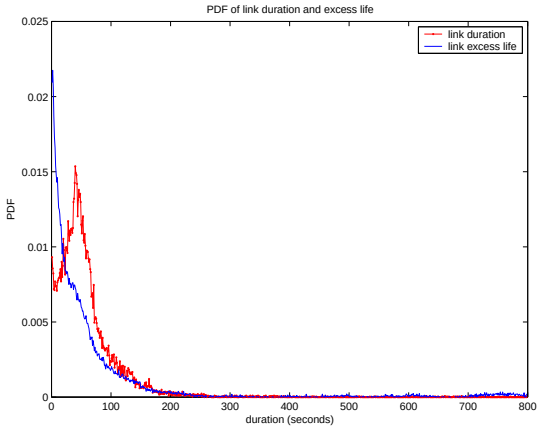

(a) RPGM with AODV

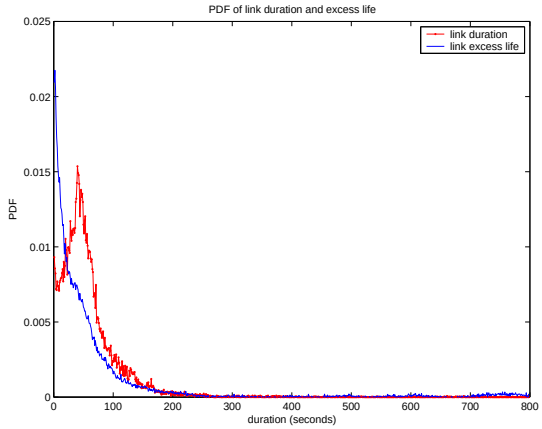

(b) RPGM with DSR

Figure 6.4: PDF of link duration and link excess life for RPGM

6.2 Path Duration CDF and Exponential Fitting

A separate empirical path duration distribution is computed for each hop count. We use the MATLAB *expfit(·)* function to exponentially fit the empirical path duration CDF. Figs. 6.5 – 6.12 show that the empirical CDFs of path duration and the exponential fitting curves with path hop count of 2 and 8. It can be seen that the fitting curves match the empirical CDFs well for path hop count of 8. This validates Theorem 2 in [20] that the path duration distribution can be well approximated by an exponential distribution for all sufficiently large path hop counts.

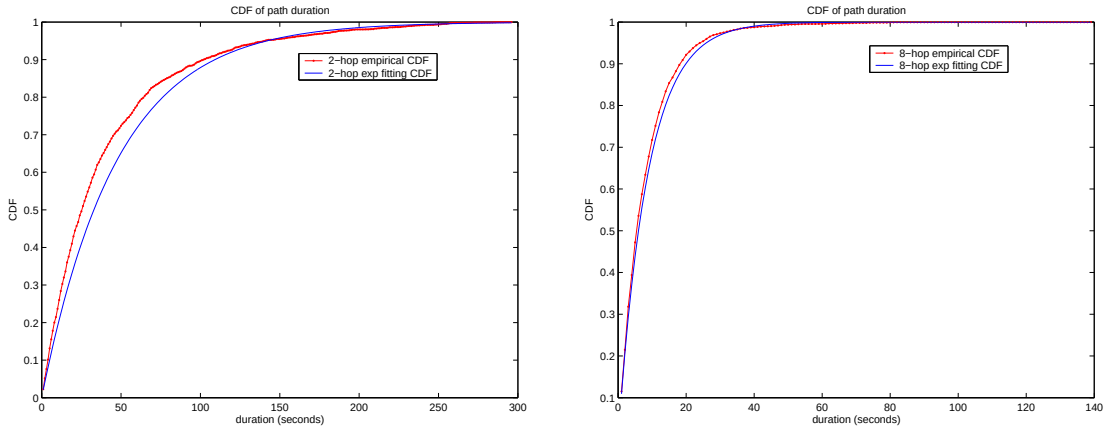

(a) 2-hop path (b) 8-hop path

Figure 6.5: CDF of path duration and MLE exponential fitting for RWP with AODV

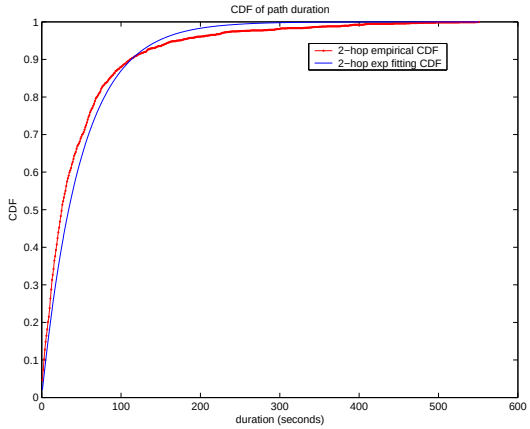

(a) 2-hop path

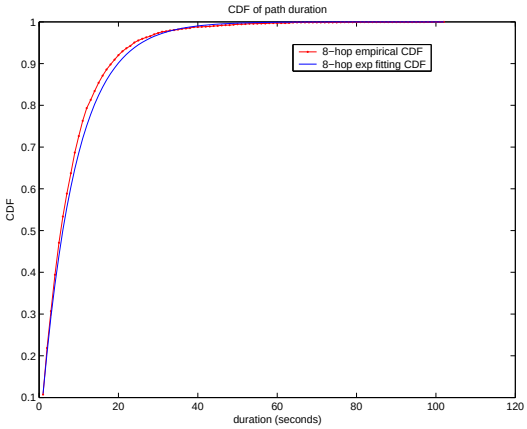

(b) 8-hop path

Figure 6.6: CDF of path duration and MLE exponential fitting for RWP with DSR

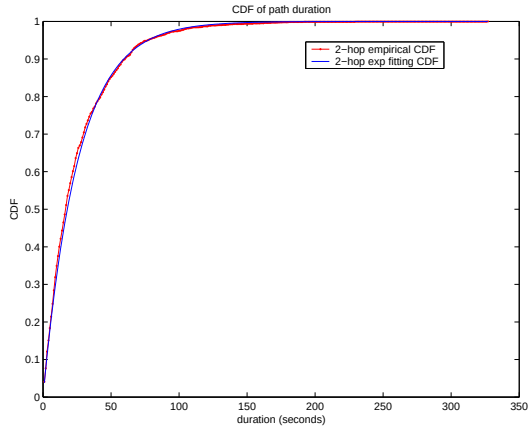

(a) 2-hop path

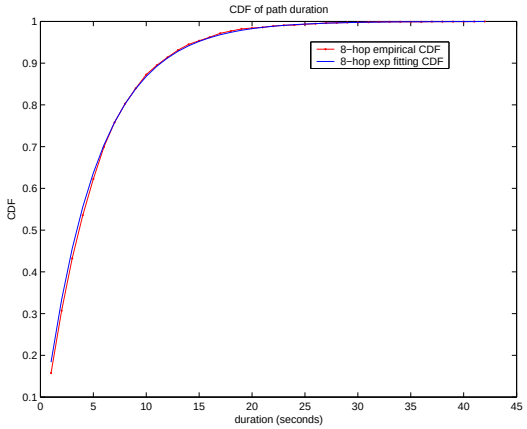

(b) 8-hop path

Figure 6.7: CDF of path duration and MLE exponential fitting for MH with AODV

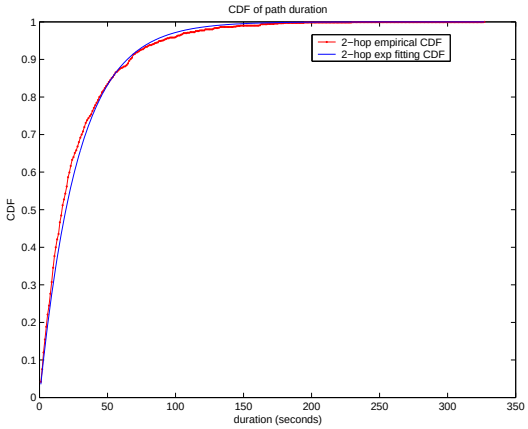

(a) 2-hop path

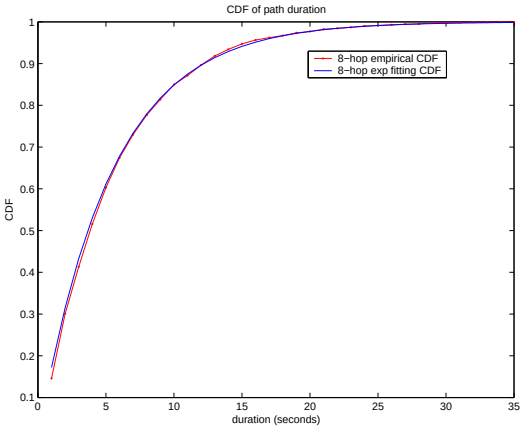

(b) 8-hop path

Figure 6.8: CDF of path duration and MLE exponential fitting for MH with DSR

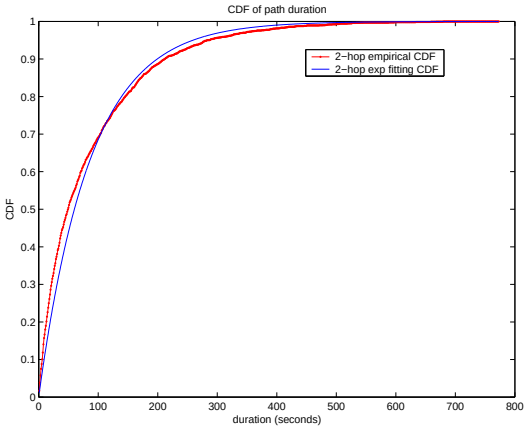

(a) 2-hop path

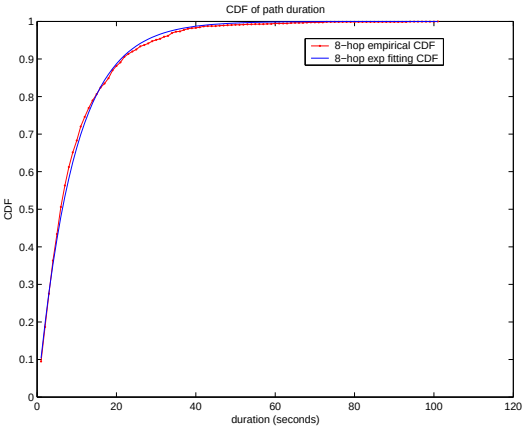

(b) 8-hop path

Figure 6.9: CDF of path duration and MLE exponential fitting for FW with AODV

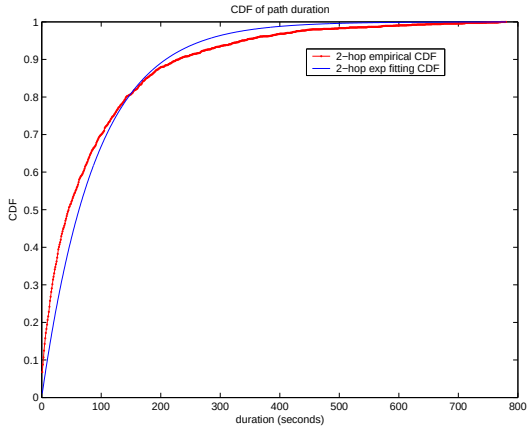

(a) 2-hop path

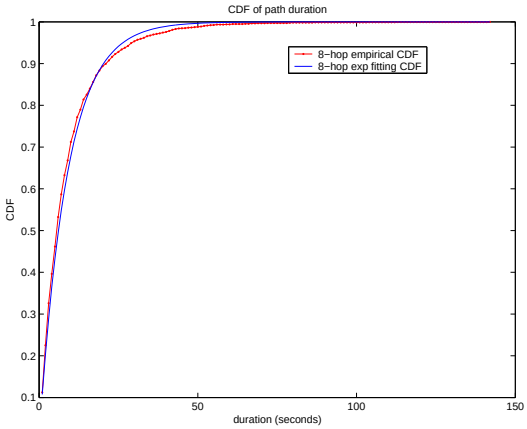

(b) 8-hop path

Figure 6.10: CDF of path duration and MLE exponential fitting for FW with DSR

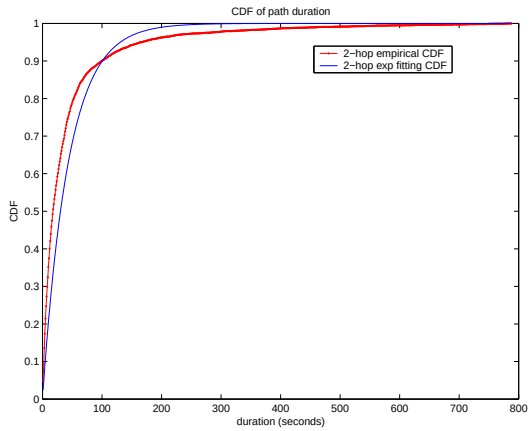

(a) 2-hop path

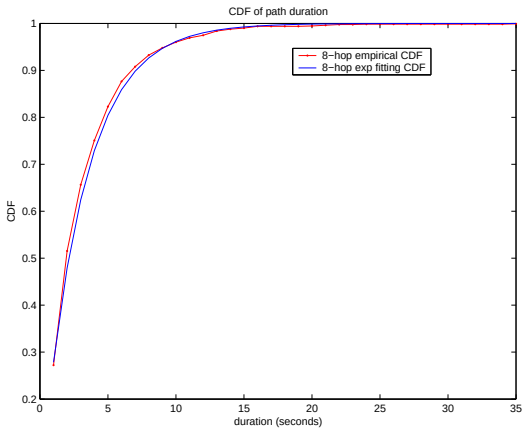

(b) 8-hop path

Figure 6.11: CDF of path duration and MLE exponential fitting for RPGM with AODV

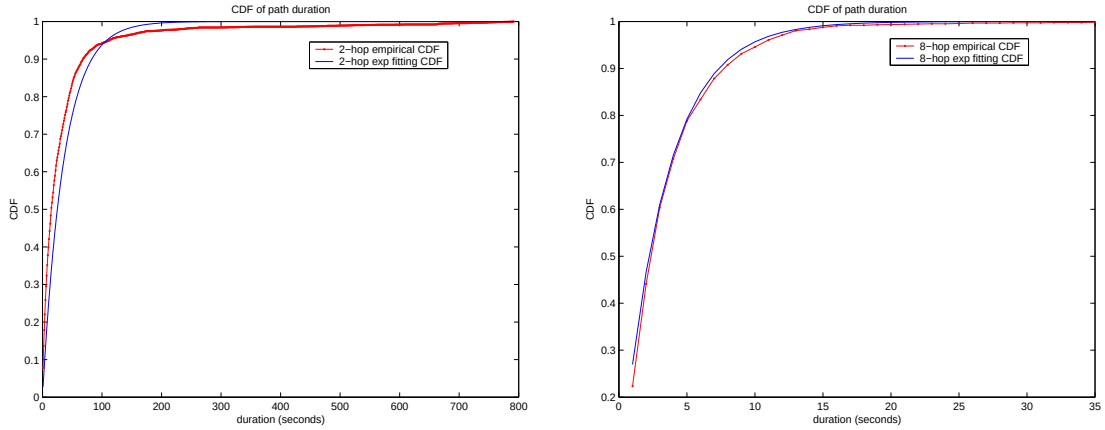

(a) 2-hop path (b) 8-hop path

Figure 6.12: CDF of path duration and MLE exponential fitting for RPGM with DSR

In order to quantify the goodness of the exponential fitting, we compute the fitting error between the empirical CDF and the exponential fitting curve, using Kolmogorov-Smirnov goodness-of-fit test (K-S test) as follows: [1]

$$sup_{x \geq 0} \Big| F_{emp}(x) - F_{mle}(x) \Big|, \tag{6.1}$$

where F_{emp} is the empirical CDF of path duration and F_{mle} is the MLE exponential fitting. The exponential fitting parameters and errors computed by (6.1) are listed in Table 6.3 and 6.4, respectively, for different path hop counts under all eight scenarios. In each column (except the leftmost column), the numbers in bold face are fitting parameters, and the numbers inside parentheses are fitting errors.

[1] We compute the difference only at the time instant when we have data.

Table 6.3: Exponential Fitting Parameter and Error I – AODV

hop count	RWP with AODV	MH with AODV	FW with AODV	RPGM with AODV
1	**0.0095** (0.1160)	**0.0155** (0.0503)	**0.0071** (0.1552)	**0.0056** (0.1592)
2	**0.0211** (0.0976)	**0.0384** (0.0366)	**0.0171** (0.1301)	**0.0390** (0.1272)
3	**0.0352** (0.0785)	**0.0654** (0.0338)	**0.0341** (0.1194)	**0.0712** (0.0992)
4	**0.0508** (0.0783)	**0.0915** (0.0316)	**0.0457** (0.0721)	**0.1178** (0.0894)
5	**0.0714** (0.0517)	**0.1129** (0.0311)	**0.0539** (0.0543)	**0.1665** (0.0707)
6	**0.0879** (0.0505)	**0.1349** (0.0296)	**0.0694** (0.0474)	**0.2279** (0.0561)
7	**0.1048** (0.0433)	**0.1608** (0.0289)	**0.0861** (0.0391)	**0.2964** (0.0392)
8	**0.1156** (0.0354)	**0.2029** (0.0266)	**0.1019** (0.0302)	**0.3263** (0.0360)
9	**0.1362** (0.0312)	**0.2329** (0.0263)	**0.1093** (0.0294)	**0.4011** (0.0351)
10	**0.1485** (0.0295)	**0.2375** (0.0226)	**0.1311** (0.0277)	-
11	**0.1593** (0.0284)	**0.2436** (0.0196)	**0.1438** (0.0261)	-
12	**0.1833** (0.0278)	**0.2685** (0.0190)	**0.1542** (0.0252)	-

Table 6.4: Exponential Fitting Parameter and Error II – DSR

hop count	RWP with DSR	MH with DSR	FW with DSR	RPGM with DSR
1	**0.0101** (0.1051)	**0.0177** (0.0503)	**0.0078** (0.1548)	**0.0068** (0.1981)
2	**0.0214** (0.0865)	**0.0371** (0.0452)	**0.0182** (0.1416)	**0.0541** (0.1226)
3	**0.0355** (0.0772)	**0.0682** (0.0357)	**0.0337** (0.1199)	**0.0668** (0.1121)
4	**0.0484** (0.0708)	**0.0874** (0.0343)	**0.0541** (0.0929)	**0.0986** (0.0935)
5	**0.0681** (0.0633)	**0.1113** (0.0329)	**0.0638** (0.0574)	**0.1445** (0.0792)
6	**0.0840** (0.0527)	**0.1330** (0.0327)	**0.0715** (0.0466)	**0.1978** (0.0641)
7	**0.1031** (0.0471)	**0.1535** (0.0298)	**0.0844** (0.0418)	**0.2483** (0.0473)
8	**0.1159** (0.0422)	**0.1906** (0.0279)	**0.1008** (0.0405)	**0.3089** (0.0423)
9	**0.1309** (0.0393)	**0.1989** (0.0278)	**0.1135** (0.0388)	**0.3327** (0.0379)
10	**0.1465** (0.0353)	**0.2204** (0.0238)	**0.1234** (0.0379)	-
11	**0.1671** (0.0347)	**0.2389** (0.0211)	**0.1495** (0.0296)	-
12	**0.1710** (0.0294)	**0.2496** (0.0197)	**0.1646** (0.0263)	-

As one can see, the fitting accuracy improves with increasing path hop count. For all four mobility models, the fitting error is less than 0.05 when path hop count is larger than 6. Furthermore, the fitting error is the smallest under the MH model. In fact, the fitting error is smaller than 0.05 for path hop count larger than 1 under MH.

6.3 Relationship between the Expected Path Duration and the Expected Link Durations

The theoretical analysis in [20] suggests that when the path hop count is large enough, the inverse of the expected path duration is approximately given by the sum of the inverses of the expected link durations along the path. In order to study how quickly these parameters converge, we plot the ratio of the inverse of the expected path duration to the sum of the inverses of the expected link durations along the path in Figs. 6.13 – 6.16. Clearly the ratio does not approach 1 even for path hop count of 12 for RW, MH and FW or 9 for RPGM with both AODV and DSR. However, they show that the ratio decreases after 9 hops for RWP and 5 hops for MH. For FW and RPGM, such a decrease does not take place for path hop count up to 12. We also note that the ratio in all plots is always larger than 1, *i.e.,* the inverse of the expected path duration is always larger than the sum of the inverses of the expected link durations along the path. This suggests that we overestimate the expected path duration when the sum of inverses of the expected link durations along a path is used to estimate the expected path duration.

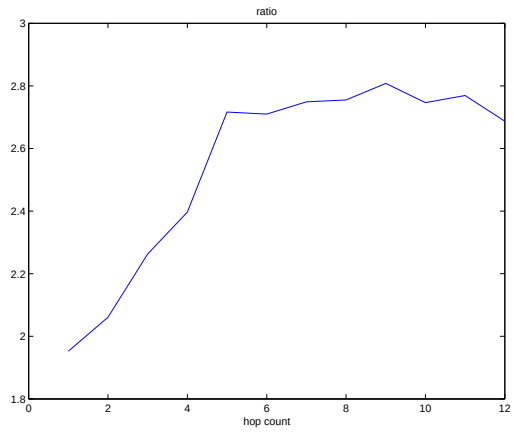

(a) RWP with AODV

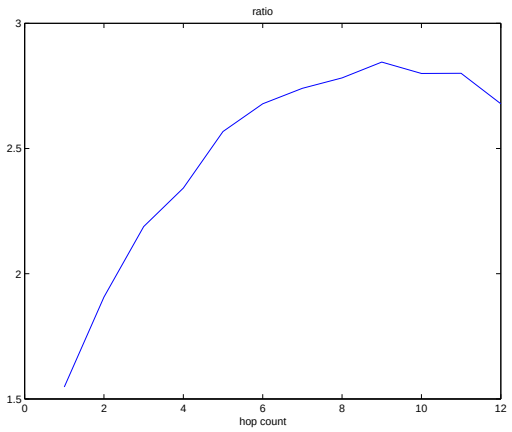

(b) RWP with DSR

Figure 6.13: Ratio of inverse of average path duration to sum of inverse of average link durations along the path for RWP

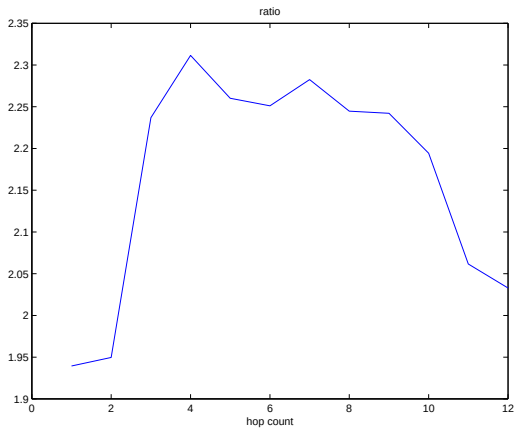

(a) MH with AODV

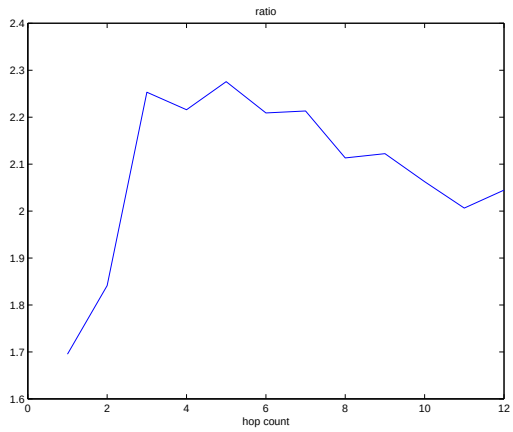

(b) MH with DSR

Figure 6.14: Ratio of inverse of average path duration to sum of inverse of average link durations along the path for MH

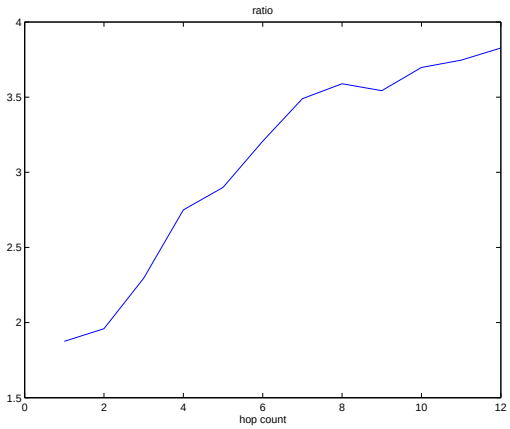

(a) FW with AODV

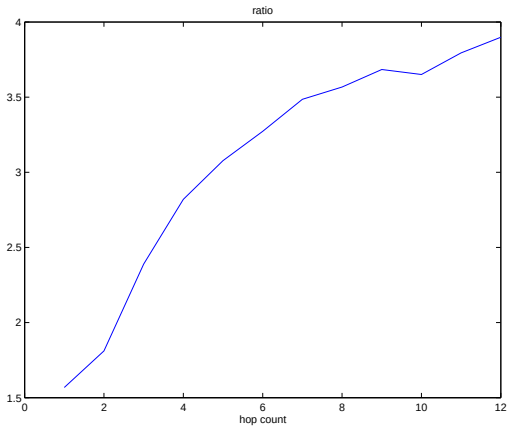

(b) FW with DSR

Figure 6.15: Ratio of inverse of average path duration to sum of inverse of average link durations along the path for FW

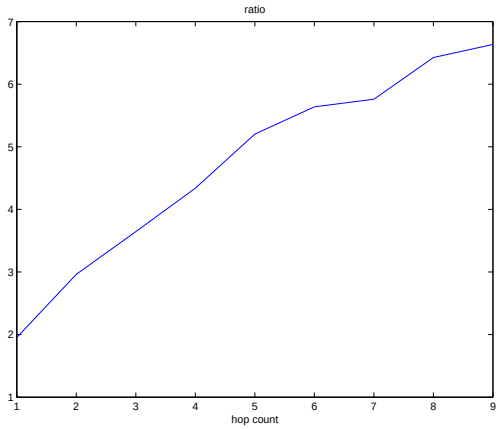

(a) RPGM with AODV

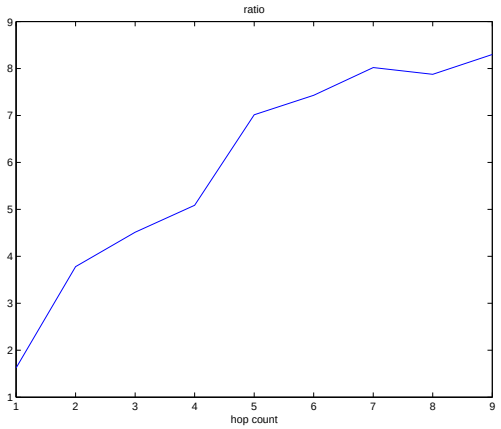

(b) RPGM with DSR

Figure 6.16: Ratio of inverse of average path duration to sum of inverse of average link durations along the path for RPGM

6.4 Dependence of Link Excess Lives

We compute the correlation coefficients of link excess lives to quantify the dependence level of link excess lives along a path. The correlation coefficients are computed for each hop distance between the links. The results are plotted in Figs. 6.17 – 6.20. The plots suggest there are some dependence in link excess lives for all scenarios. However, the dependence is mostly limited to neighboring links for RWP, MH, and FW models, and non-neighboring links exhibit very weak dependence. For RPGM, the dependence is non-negligible for hop distance less than 5. This may be because of the correlation of speeds and locations between the nodes in a group. However, the dependence does decrease as hop distance increases [2]. These suggest that the assumptions introduced in [20] are likely to hold in practice and the distribution of path duration will be approximately given by an exponential distribution if the path hop count is sufficiently large.

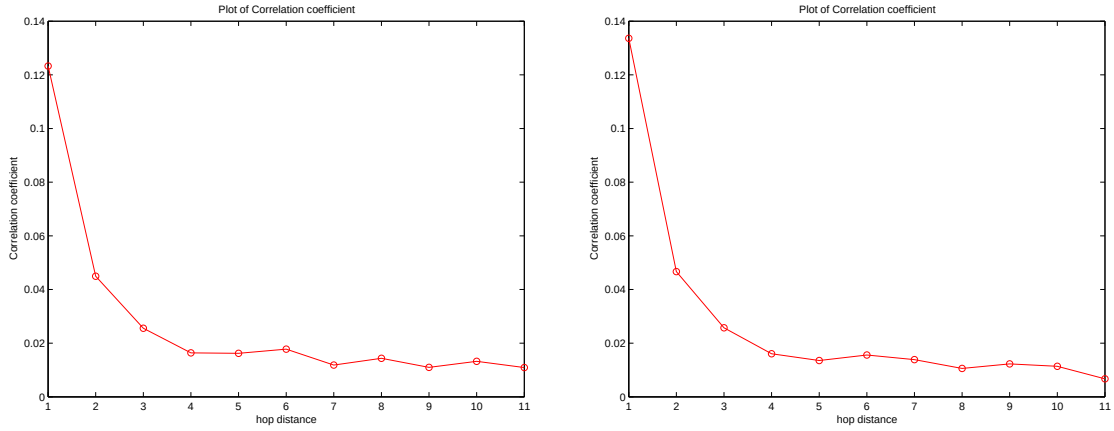

(a) RWP with AODV

(b) RWP with DSR

Figure 6.17: Correlation coefficient as a function of hop distance for RWP

[2]For MH with DSR, Fig. 6.18(b) shows the correlation coefficients are small when the hop distance is larger than 1. But there is no clearly decreasing trend with increasing hop distance. This may be because of the noise in the measurement and the limited number of data collected.

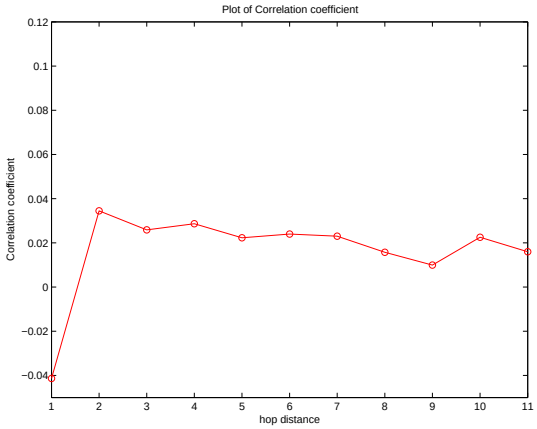

(a) MH with AODV

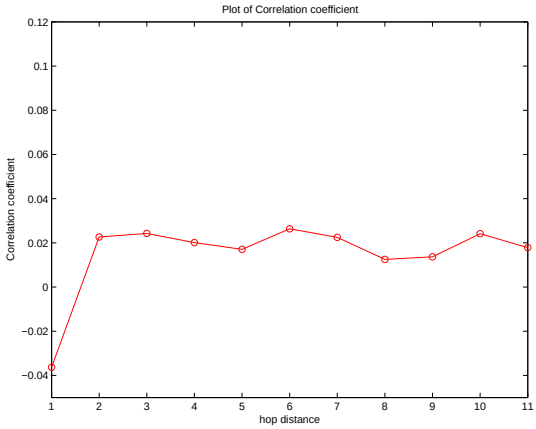

(b) MH with DSR

Figure 6.18: Correlation coefficient as a function of hop distance for MH

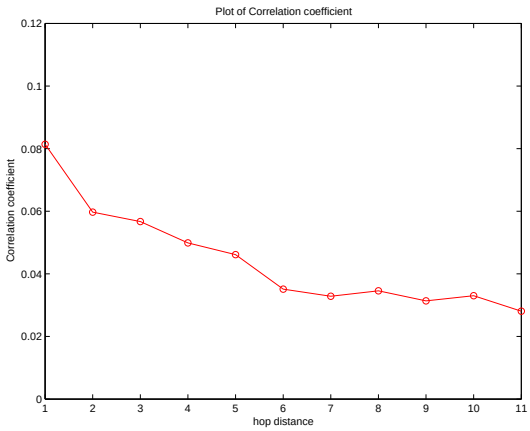

(a) FW with AODV

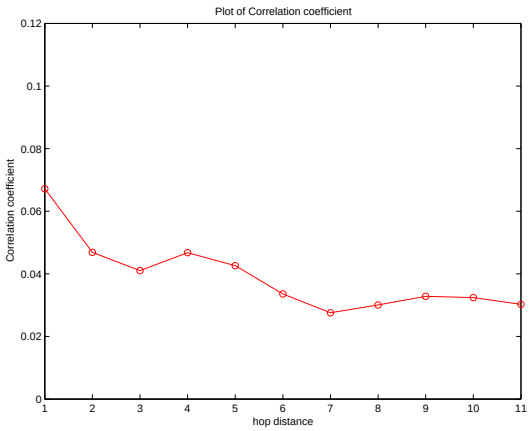

(b) FW with DSR

Figure 6.19: Correlation coefficient as a function of hop distance for FW

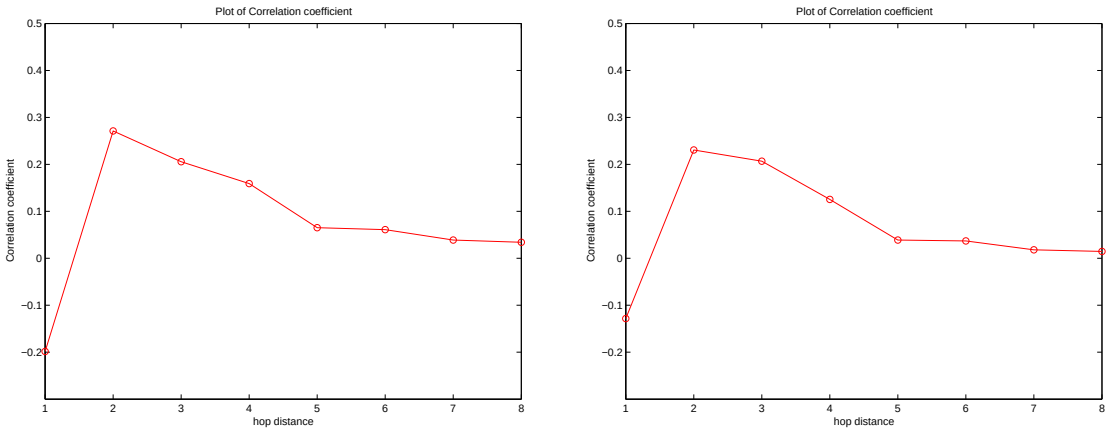

(a) RPGM with AODV (b) RPGM with DSR

Figure 6.20: Correlation coefficient as a function of hop distance for RPGM

6.5 Validation of Assumptions

6.5.1 Validation of the condition $D(u_n)$

The condition $D(u_n)$ defined in (2.5) describes the manner in which the dependence of link excess lives decays as the hop distance between links increases. Due to the limited domain size, the maximum hop count obtained from the simulations is 12. Thus, we can not fully validate the condition $D(u_n)$. However, in the following, we argue (in a somewhat imprecise manner) that the condition $D(u_n)$ is likely to hold in large scale networks.

From the observation of the correlation coefficients plotted in Figs. 6.17 – 6.20, we find that the dependence between link excess lives decreases quickly with hop distance. Thus, the dependence is the strongest between the links that are closest (in terms of hop distance) from the two sets of links, and one can argue that the level of dependence between the two sets can be inferred (to some extent) from that between the excess lives of the two closet links.

We show that indeed the dependence measured by the difference between joint

CDF and the product of the marginal CDFs of two link excess lives decreases quickly with hop distance. This seems to indicate that these two link excess lives become (almost) independent with increasing hop distance, and thus suggests that the two sets of link excess lives become independent as their hop distance increases, *i.e.,* the condition $D(u_n)$ is likely to hold.

Here, we use the difference as follows:

$$|P[X_i^{(n)} \leq x_1, X_j^{(n)} \leq x_2] - P[X_i^{(n)} \leq x_1]P[X_j^{(n)} \leq x_2]| \tag{6.2}$$

for any $x_1, x_2 \geq 0$, where $X_i^{(n)}$ and $X_j^{(n)}$ are the excess lives of two links in a path with $1 \leq i, j \leq H(n)$.

Figs. 6.21 – 6.28 plot the difference

$$\left|\mathbf{P}\left[X_\ell \leq x_1, X_{\ell+k} \leq x_2\right] - \mathbf{P}\left[X_\ell \leq x_1\right]\mathbf{P}\left[X_{\ell+k} \leq x_2\right]\right|$$

(we remove superscript (n) here without causing any confusion) for hop distance $k = 1$, 3, 5, 7. It is clear that the difference in (6.2) decreases as the hop distance increases for all scenarios. This suggests that two link excess lives become independent as their hop distance increases. This suggests that the condition $D(u_n)$ is likely to hold in large scale networks.

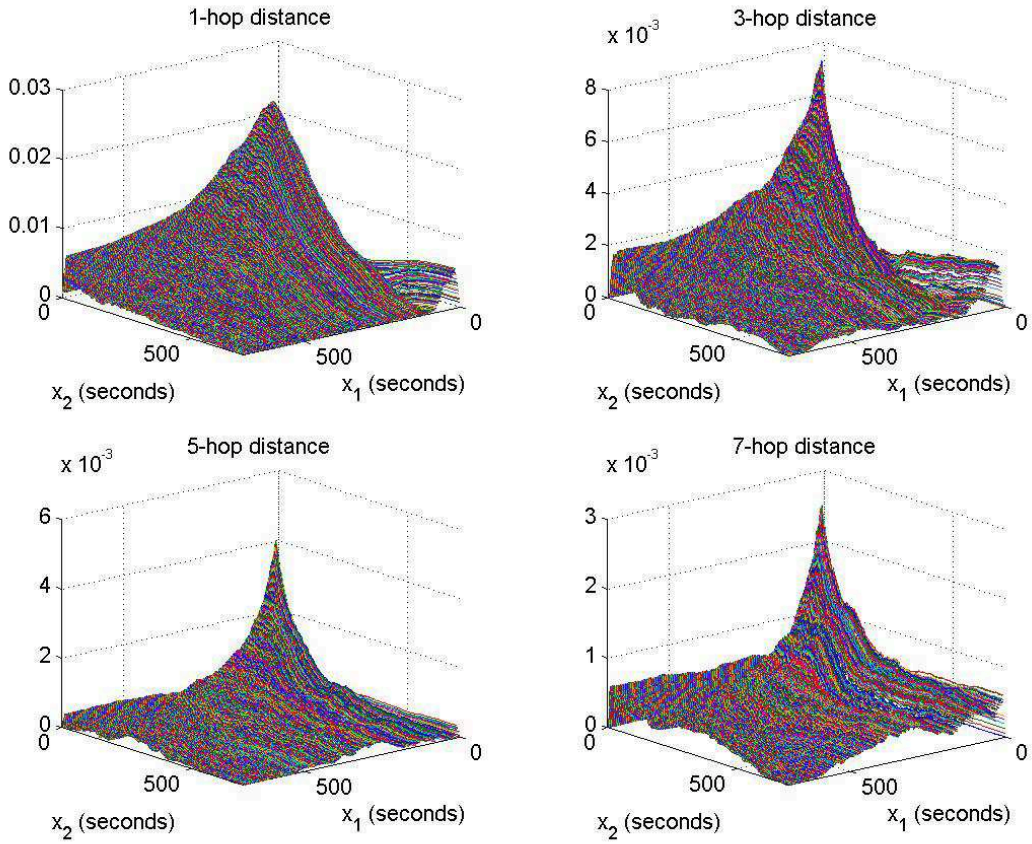

Figure 6.21: Plot of $\left|\mathbf{P}\left[X_i \leq x_1, X_{i+k} \leq x_2\right] - \mathbf{P}\left[X_i \leq x_1\right] \mathbf{P}\left[X_{i+k} \leq x_2\right]\right|$ where $k = 1, 3, 5, 7$ for RWP with AODV

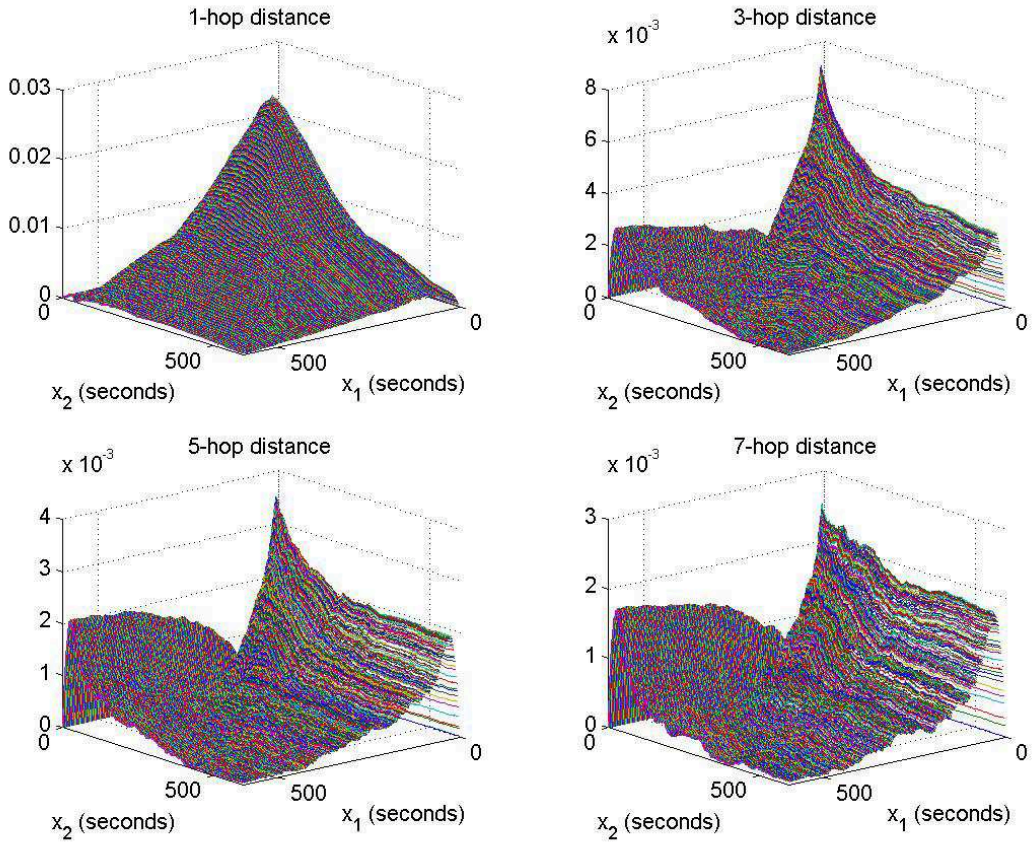

Figure 6.22: Plot of $\left|\mathbf{P}\left[X_i \leq x_1, X_{i+k} \leq x_2\right] - \mathbf{P}\left[X_i \leq x_1\right] \mathbf{P}\left[X_{i+k} \leq x_2\right]\right|$ where $k = 1, 3, 5, 7$ for RWP with DSR

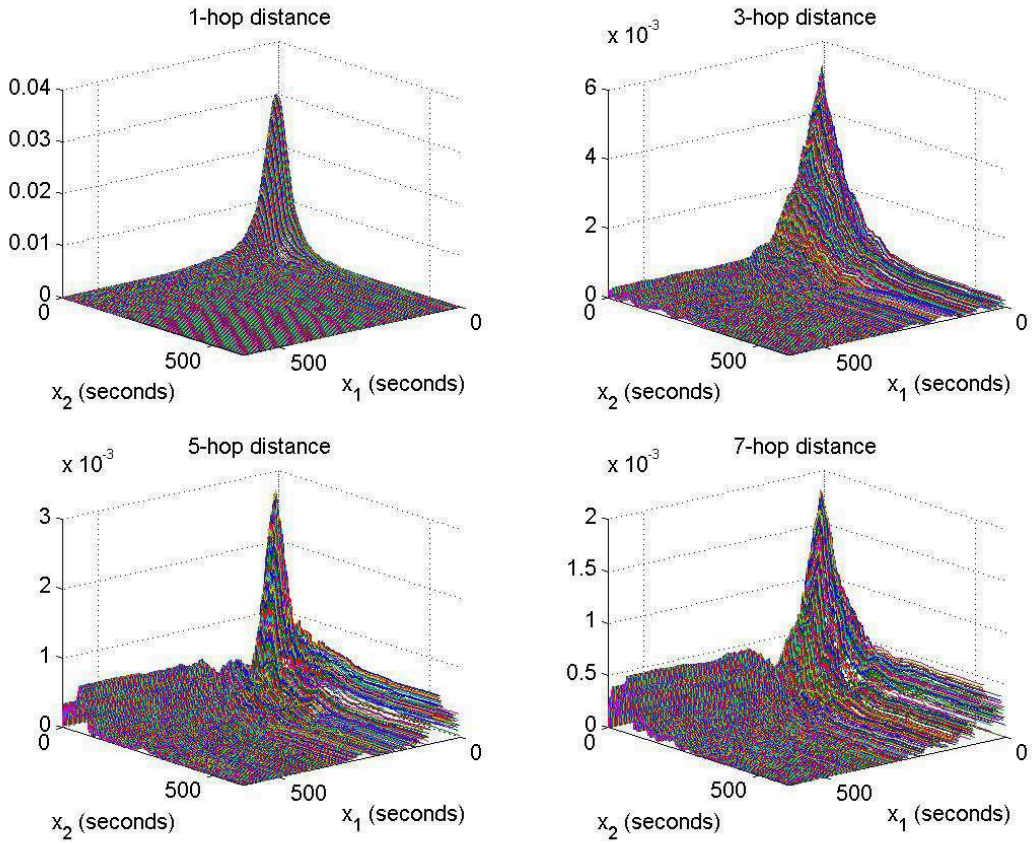

Figure 6.23: Plot of $\left|\mathbf{P}\left[X_i \leq x_1, X_{i+k} \leq x_2\right] - \mathbf{P}\left[X_i \leq x_1\right] \mathbf{P}\left[X_{i+k} \leq x_2\right]\right|$ where $k = 1, 3, 5, 7$ for MH with AODV

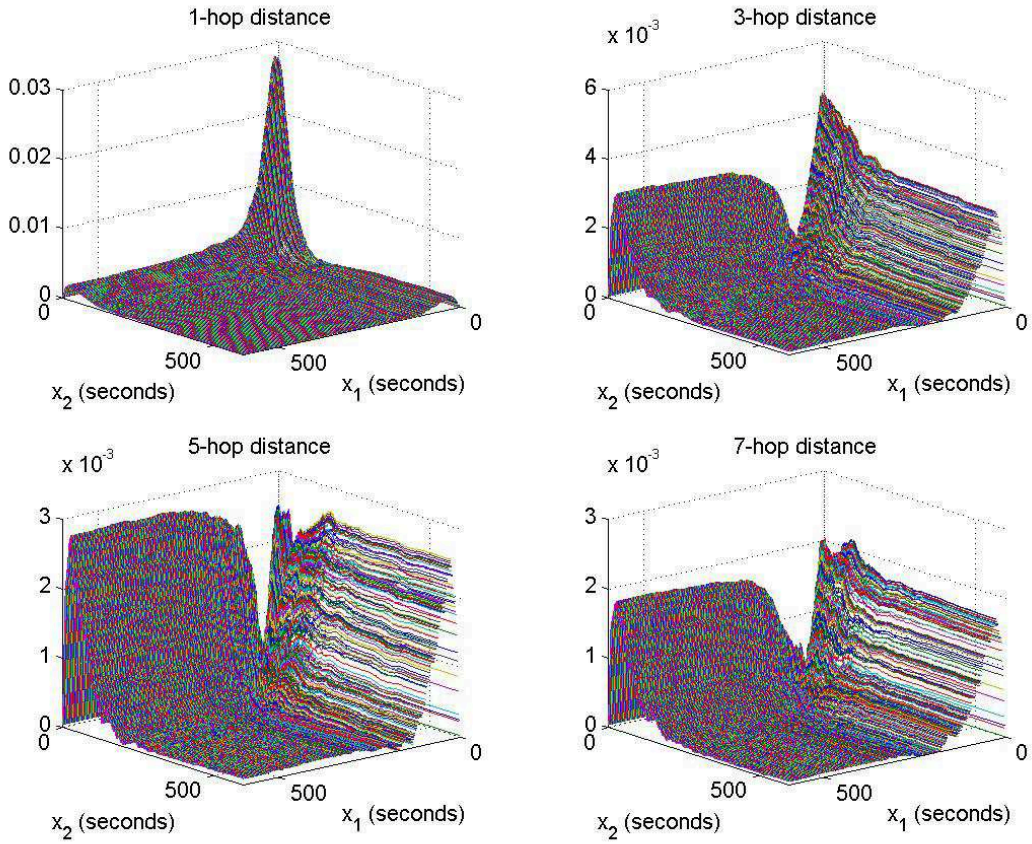

Figure 6.24: Plot of $\left|\mathbf{P}\left[X_i \leq x_1, X_{i+k} \leq x_2\right] - \mathbf{P}\left[X_i \leq x_1\right] \mathbf{P}\left[X_{i+k} \leq x_2\right]\right|$ where $k = 1, 3, 5, 7$ for MH with DSR

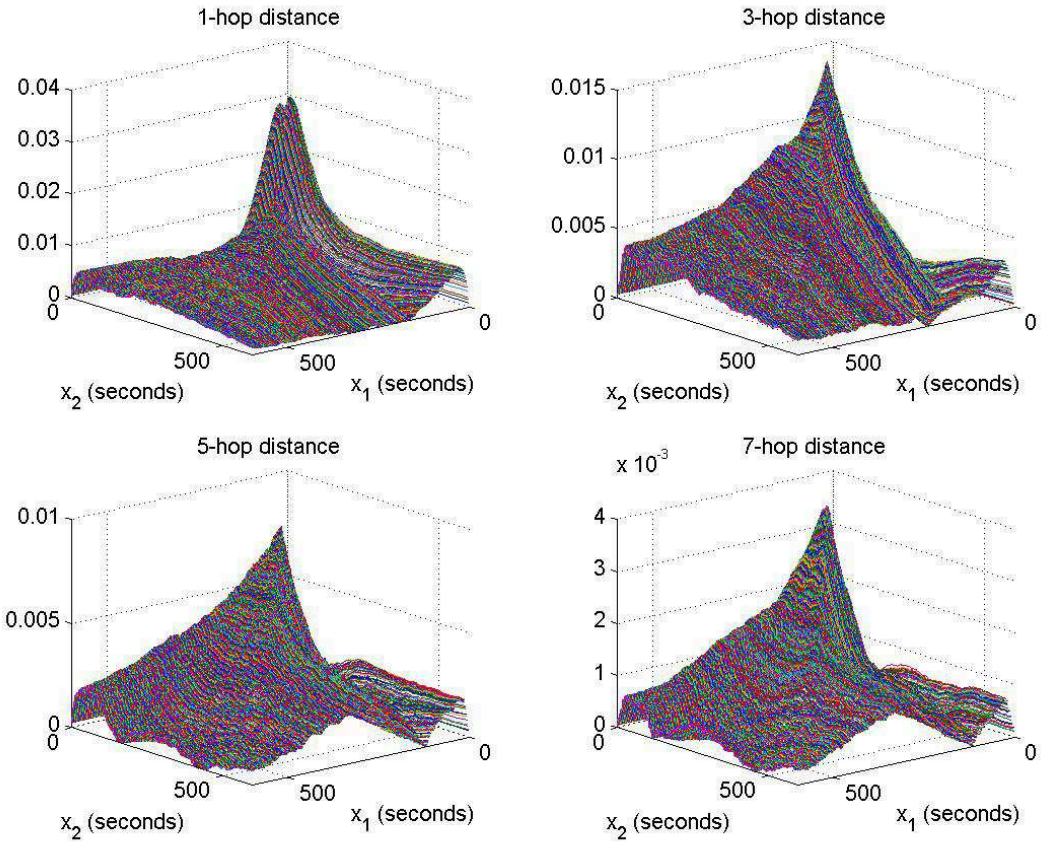

Figure 6.25: Plot of $\left|\mathbf{P}\left[X_i \leq x_1, X_{i+k} \leq x_2\right] - \mathbf{P}\left[X_i \leq x_1\right] \mathbf{P}\left[X_{i+k} \leq x_2\right]\right|$ where $k = 1, 3, 5, 7$ for FW with AODV

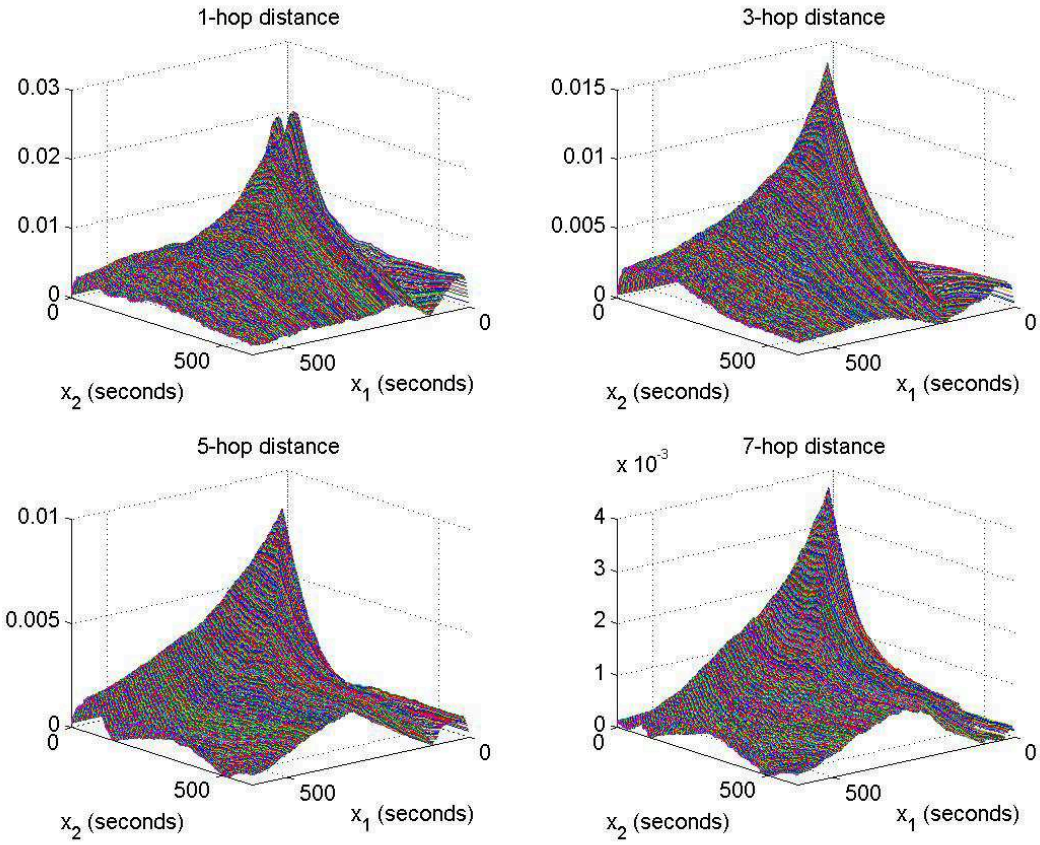

Figure 6.26: Plot of $\left|\mathbf{P}\left[X_i \leq x_1, X_{i+k} \leq x_2\right] - \mathbf{P}\left[X_i \leq x_1\right] \mathbf{P}\left[X_{i+k} \leq x_2\right]\right|$ where $k = 1, 3, 5, 7$ for FW with DSR

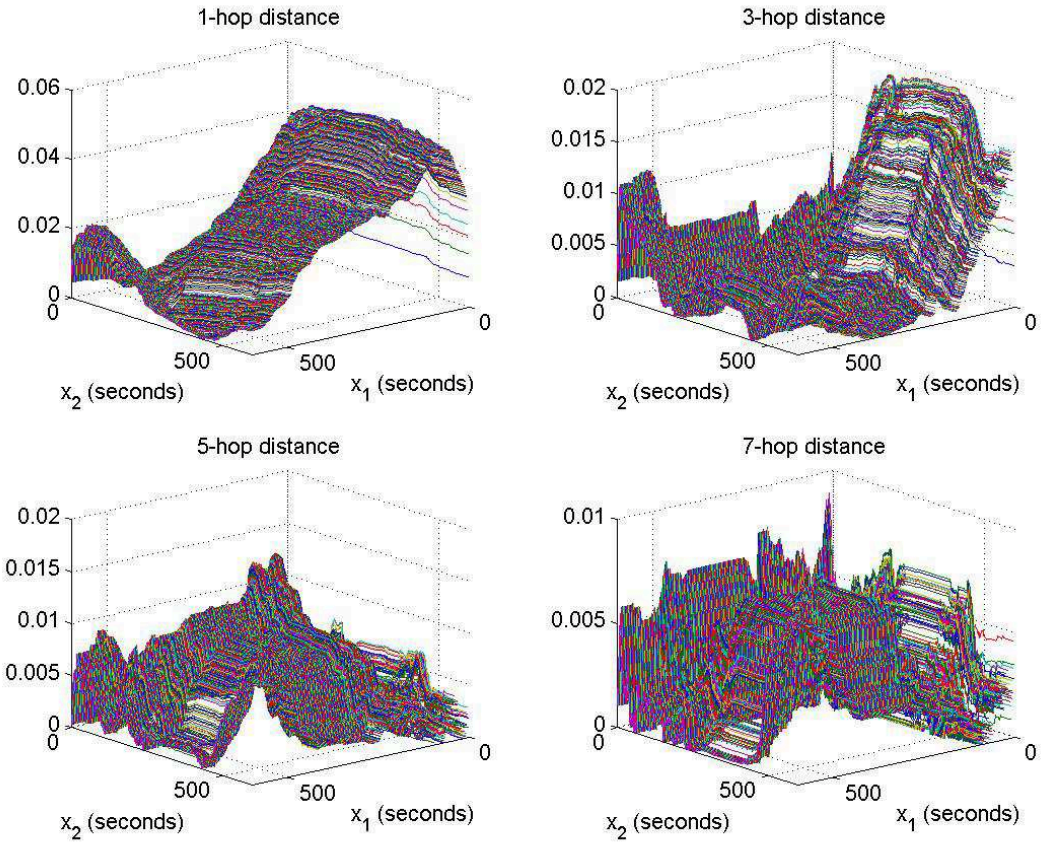

Figure 6.27: Plot of $\left|\mathbf{P}\left[X_i \leq x_1, X_{i+k} \leq x_2\right] - \mathbf{P}\left[X_i \leq x_1\right] \mathbf{P}\left[X_{i+k} \leq x_2\right]\right|$ where $k = 1, 3, 5, 7$ for RPGM with AODV

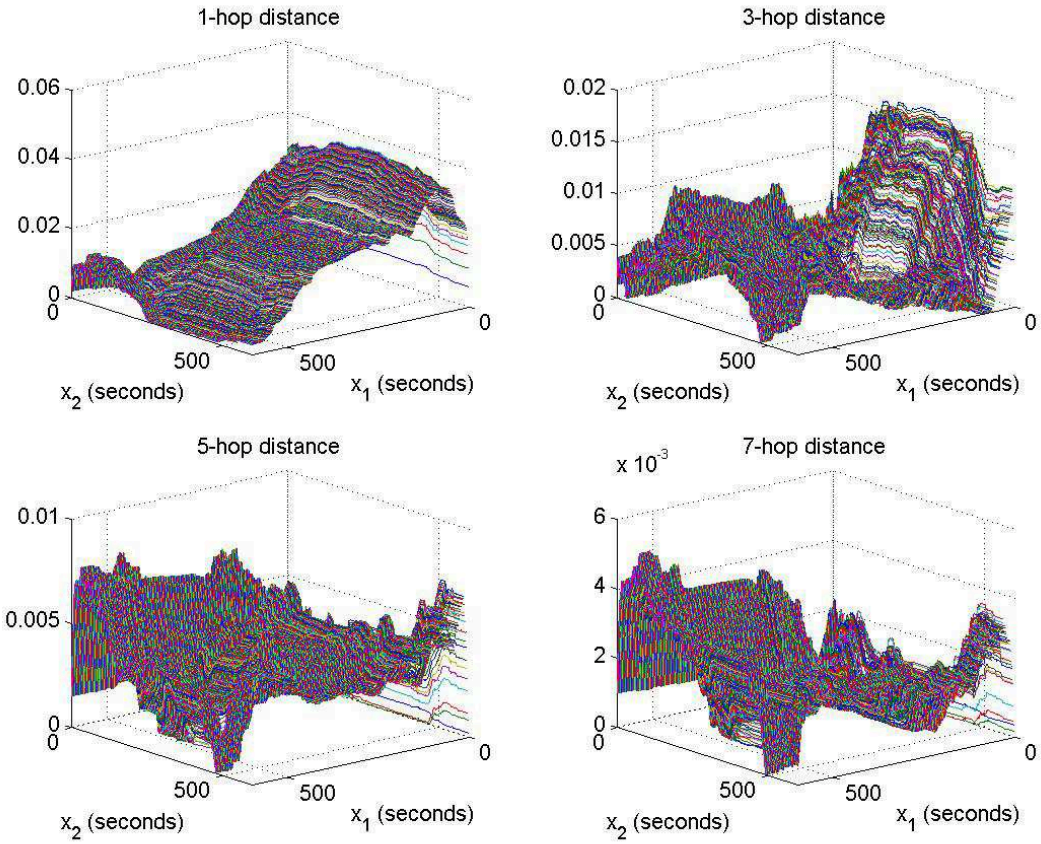

Figure 6.28: Plot of $\left|\mathbf{P}\left[X_i \leq x_1, X_{i+k} \leq x_2\right] - \mathbf{P}\left[X_i \leq x_1\right] \mathbf{P}\left[X_{i+k} \leq x_2\right]\right|$ where $k = 1, 3, 5, 7$ for RPGM with DSR

6.5.2 Validation of the condition $D'(u_n)$

A sufficient condition for the condition $D'(u_n)$ with $u_n = H(n)/x$ for any $x \in (0, \infty)$ is given in (2.7). We can rewrite (2.7) as

$$\lim_{n\to\infty} \left(\left\lfloor \frac{H(n)}{k} \right\rfloor^2 \cdot \sup_{i,i' \in I_{k,j}^{(n)}: i<i'} P[X_i^{(n)} < \frac{x}{H(n)}] \cdot P[X_{i'}^{(n)} < \frac{x}{H(n)} \big| X_i^{(n)} < \frac{x}{H(n)}] \right) = o\left(\frac{1}{k}\right) \tag{6.3}$$

for all $j = 1, \ldots, k$.

By replacing x with $x/H(n)$ in the CDF of the link excess life given in (2.2), we have

$$P[X_i^{(n)} < \frac{x}{H(n)}] = \frac{1}{m(G_\ell^{(n)})} \int_0^{\frac{x}{H(n)}} (1 - G_\ell^{(n)}(y))\, dy \tag{6.4}$$

As mentioned earlier, a sufficient condition for Assumption 3 introduced in Chapter 2 (or Assumption 5 in [20]) is that there exists some arbitrarily small positive constant ε such that $m(G_\ell^{(n)}) \geq \varepsilon$ for all $n = 1, 2, \ldots$ and $\ell = 1, 2, \ldots, H(n)$, *i.e.,* $m(G_\ell^{(n)})$ is lower bounded by a positive constant. Putting these together, we have

$$P[X_i^{(n)} < \frac{x}{H(n)}] = \frac{c'}{H(n)} + o\left(\frac{1}{H(n)}\right) \tag{6.5}$$

where c' is some finite positive constant.

As $n \to \infty$, $H(n)/k \to \infty$. Hence, $\lfloor H(n)/k \rfloor \simeq H(n)/k$ for large n, and we can approximate $\lfloor H(n)/k \rfloor$ by $H(n)/k$. Combining (6.3) and (6.5), we get

$$\lim_{n\to\infty} \left((c' + o(1)) \frac{H(n)}{k^2} \sup_{i,i' \in I_{k,j}^{(n)}: i<i'} P[X_{i'}^{(n)} < \frac{x}{H(n)} \big| X_i^{(n)} < \frac{x}{H(n)}] \right) = o\left(\frac{1}{k}\right) \tag{6.6}$$

A sufficient condition for (6.6) to hold is that

$$P[X_{i'}^{(n)} < \frac{x}{H(n)} \big| X_i^{(n)} < \frac{x}{H(n)}] = \frac{c''_{ii'}}{H(n)} + o\left(\frac{1}{H(n)}\right) \tag{6.7}$$

for all $i, i' \in I_{k,j}^{(n)}$ such that $i < i'$, where $c''_{ii'}$ is a finite positive constant. Equation (6.7) simply says that the probability $P[X_{i'}^{(n)} < \frac{x}{H(n)} \big| X_i^{(n)} < \frac{x}{H(n)}]$ behaves similarly as the

marginal CDF $P[X_i^{(n)} < \frac{x}{H(n)}]$ as $n \to \infty$ $(x/H(n) \to 0)$. In the following, we will show that this is indeed the case.

Figs. 6.29(a) – 6.36(a) plot the empirical CDFs of link excess life (*i.e.*, $P[X_\ell \leq c]$) and the conditional probabilities $P[X_{\ell+1} \leq c | X_\ell \leq c]$ (we remove superscript (n) here without causing any confusion). We also plot the same CDF and the conditional probability $P[X_{\ell+k} \leq c | X_\ell \leq c]$ for hop distance $k = 2, 4$ in Figs. 6.29(b) – 6.36(b). These figures show that the conditional probabilities and the CDFs do not coincide but are close, providing further evidence that the excess lives of two links are not independent but are weakly dependent if separated by intermediate links. Also, in all cases the conditional probability behaves similarly as CDFs as c decreases to 0. This suggests that the sufficient condition (6.7) for (6.3) holds for all scenarios.

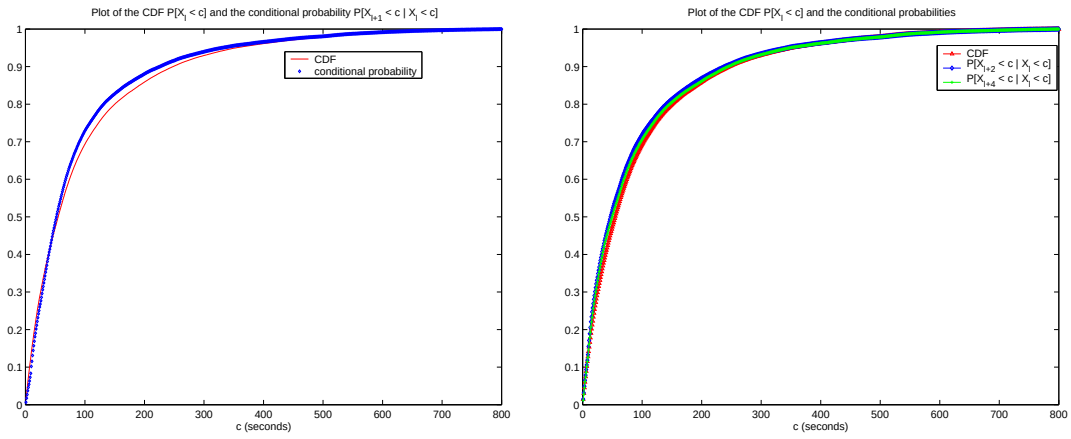

(a) $\mathbf{P}\left[X_{\ell+1} \leq c | X_\ell \leq c\right]$ (b) $\mathbf{P}\left[X_{\ell+k} \leq c | X_\ell \leq c\right]$, $k = 2, 4$

Figure 6.29: Plot of the CDF and the conditional probabilities for RWP with AODV

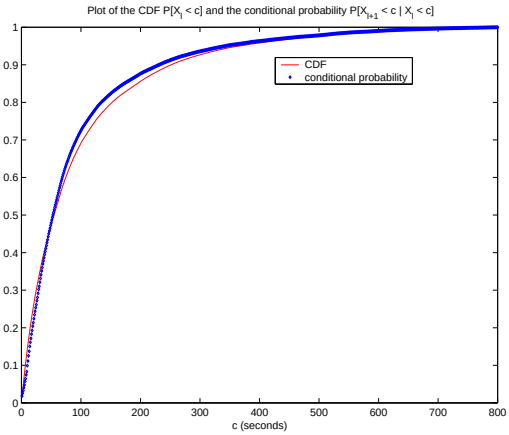

(a) $\mathbf{P}\left[X_{\ell+1} \leq c | X_{\ell} \leq c\right]$

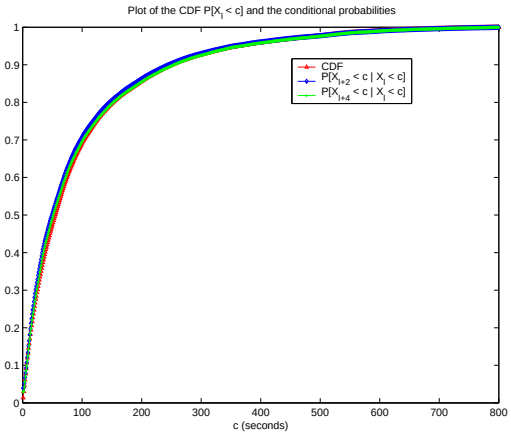

(b) $\mathbf{P}\left[X_{\ell+k} \leq c | X_{\ell} \leq c\right],\ k = 2, 4$

Figure 6.30: Plot of the CDF and the conditional probabilities for RWP with DSR

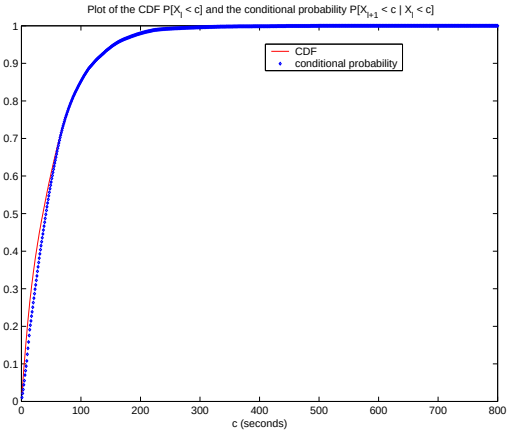

(a) $\mathbf{P}\left[X_{\ell+1} \leq c | X_{\ell} \leq c\right]$

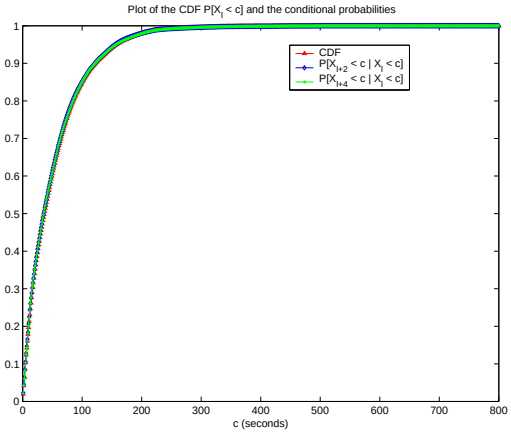

(b) $\mathbf{P}\left[X_{\ell+k} \leq c | X_{\ell} \leq c\right],\ k = 2, 4$

Figure 6.31: Plot of the CDF and the conditional probabilities for MH with AODV

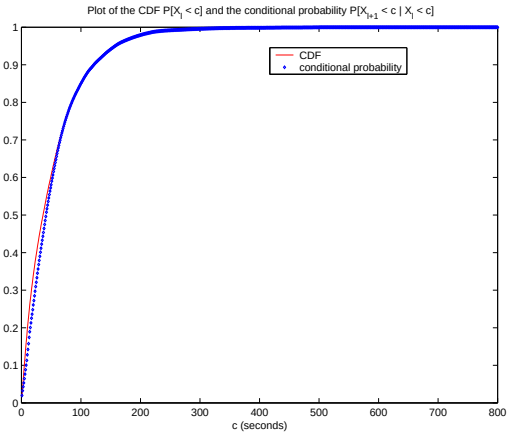

(a) $\mathbf{P}\left[X_{\ell+1} \leq c | X_{\ell} \leq c\right]$

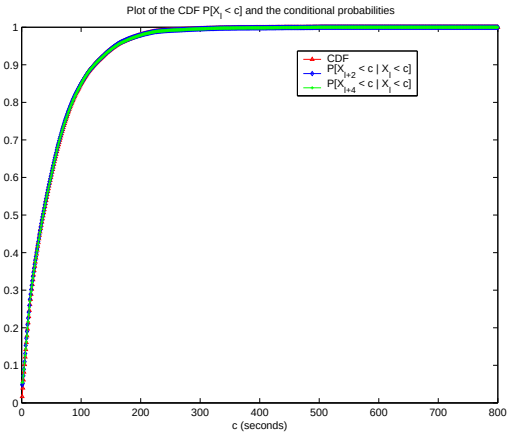

(b) $\mathbf{P}\left[X_{\ell+k} \leq c | X_{\ell} \leq c\right],\ k = 2, 4$

Figure 6.32: Plot of the CDF and the conditional probabilities for MH with DSR

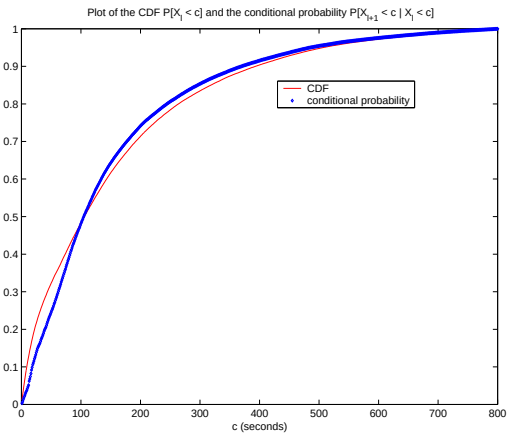

(a) $\mathbf{P}\left[X_{\ell+1} \leq c | X_{\ell} \leq c\right]$

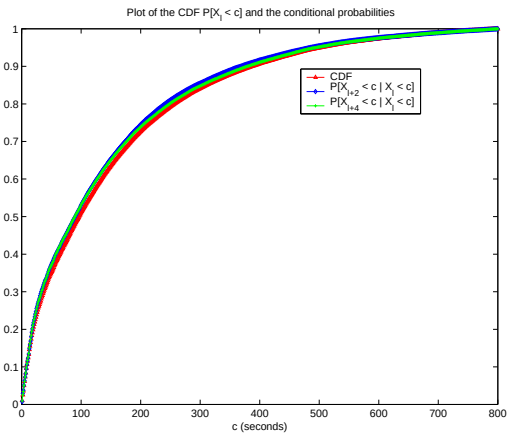

(b) $\mathbf{P}\left[X_{\ell+k} \leq c | X_{\ell} \leq c\right],\ k = 2, 4$

Figure 6.33: Plot of the CDF and the conditional probabilities for FW with AODV

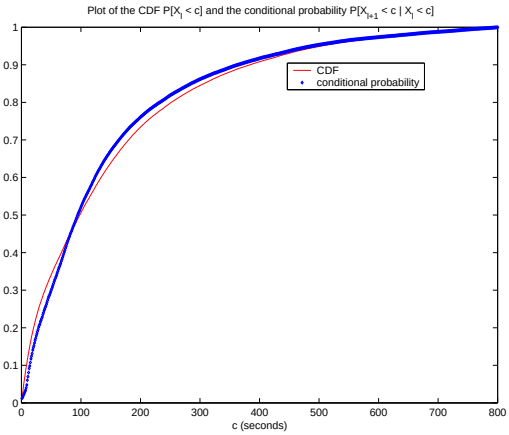

(a) $\mathbf{P}\left[X_{\ell+1} \leq c | X_{\ell} \leq c\right]$

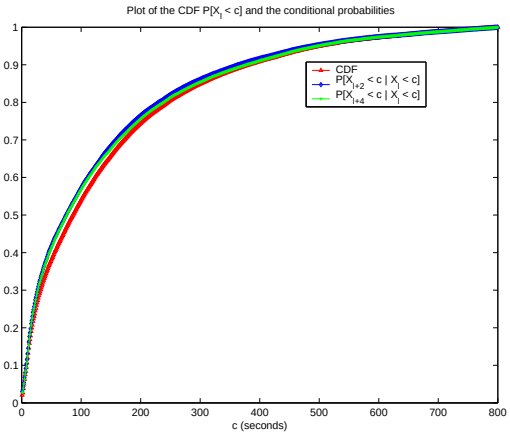

(b) $\mathbf{P}\left[X_{\ell+k} \leq c | X_{\ell} \leq c\right],\ k = 2, 4$

Figure 6.34: Plot of the CDF and the conditional probabilities for FW with DSR

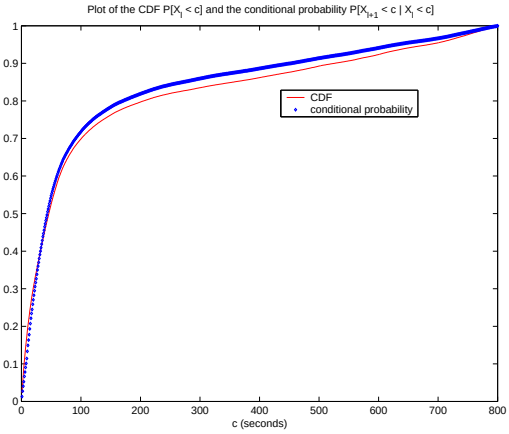

(a) $\mathbf{P}\left[X_{\ell+1} \leq c | X_{\ell} \leq c\right]$

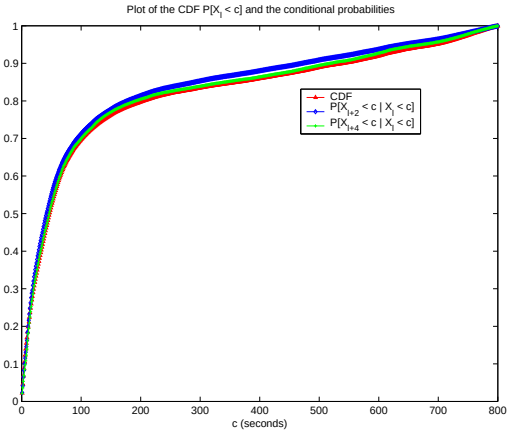

(b) $\mathbf{P}\left[X_{\ell+k} \leq c | X_{\ell} \leq c\right],\ k = 2, 4$

Figure 6.35: Plot of the CDF and the conditional probabilities for RPGM with AODV

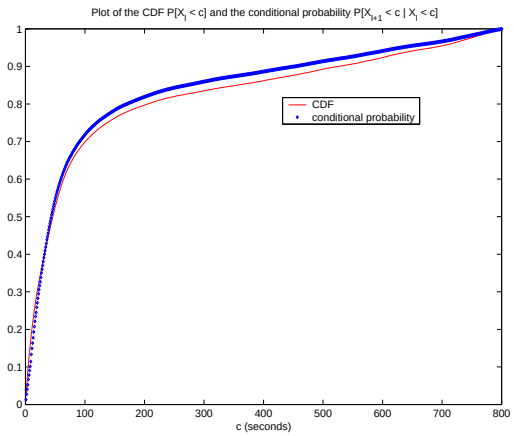

(a) $\mathbf{P}\left[X_{\ell+1} \leq c | X_\ell \leq c\right]$

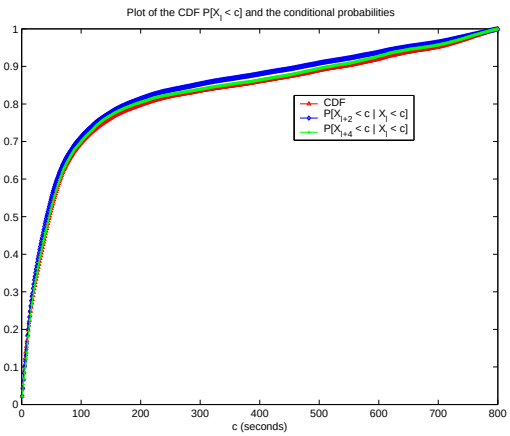

(b) $\mathbf{P}\left[X_{\ell+k} \leq c | X_\ell \leq c\right]$, $k = 2, 4$

Figure 6.36: Plot of the CDF and the conditional probabilities for RPGM with DSR

6.6 Summary and Comparison

We studied the link and path duration distributions through extensive simulations. There are two major findings: First, We find that the convergence of path duration distribution takes place quickly. In other words, even for hop counts of 5 - 7, the distribution of path duration can be well approximated by an exponential distribution. The two routing protocols used in our simulations yield similar results. Second, the inverse of the expected path duration cannot be well approximated by the sum of the inverses of the expected link durations along a path even when path hop count is equal to 12 for the RWP, MH, and FW models and 9 for the RPGM model. In fact, the expected path duration is overestimated by using the sum of the inverses of the expected link durations at least for path hop count up to 12.

For the RWP, MH, and FW models, the dependence of link excess lives is weak between non-neighboring links. For the RPGM model, the local dependence of link excess lives is non-negligible for hop distance less than 5. A sufficient condition for mixing condition $D(u_n)$ is validated for all considered scenarios. And, based on the observation

that the level of dependence of link excess lives decreases as hop distance increases, we believe that the condition $D'(U_n)$ will hold in practice for large scale networks. Specifically, simulation results show that the difference between the joint CDF of two link excess lives and the product of their marginal CDFs decreases as the hop distance between the two links increases.

Chapter 7

Conclusions and Future Work

In this thesis, we carried out simulation studies of the link and path duration distributions in a multi-hop wireless ad hoc networks. Through extensive simulations using four different mobility models and two different on-demand routing protocols, we find when the path hop count is larger than 5 or 6, the path duration can be well approximated by an exponential distribution with the fitting error less than 0.05 using KS-test. Among the four mobility models considered, the MH model gives the fastest decreasing rate of fitting error. The other three models show similar results. The two routing protocols studied here, namely AODV and DSR, do yield similar quantitative results. The inverse of the expected path duration and the sum of the inverses of the expected link durations along a path shows non-negligible difference for path hop count up to 12.

Through the computation of the correlation coefficients between link excess lives, we find that the dependence of link excess lives is quite weak for non-neighboring links under RWP, MH and FW models. For the RPGM model, the dependence is non-negligible for hop distance less than 5. A sufficient condition for the condition $D'(u_n)$ is validated for all considered scenarios. Simulation results show that the probability of one link excess life less than a positive number conditioned on the excess life of another link in the same path less than the same number behaves similarly as the CDF of that link excess life as the number decreases to 0. And, based on the observation of the level of dependence of link excess lives decreasing with increasing hop distance, we validate a condition that suggests that indeed the condition $D(u_n)$ is likely to hold in a large scale network in the cases of

all scenarios. Specifically, simulation results show that the difference between the joint CDF of two link excess lives and the product of their marginal CDFs decreases as the hop distance between the two links increases.

We plan to run simulations in a larger scale network to investigate when the inverse of an expected path duration can be accurately approximated by the sum of the inverse of the expected link durations along a path. We will further investigate the same issues under other various settings, *e.g.,* different network size, node speed range, mobility models (*e.g.,* obstacle mobility models or those generated from real life systems), routing protocols (*e.g.,* TORA or ABR), etc. These will help us better understand the link and path duration distributions in MANETs.

A new path selection scheme is proposed in [20]. In the scheme, a path with the largest expected duration is selected by a source for packet transmission. An expected path duration is estimated using the relationship between the expected path duration and the expected durations of the links along the path. Our simulation results suggest that an expected path duration is overestimated by using the sum of the inverses of the expected durations of the links along the path at least for path hop count up to 12 under RWP, MH, and FW models or 9 under RPGM model. Therefore, the new scheme may need to compensate for the discrepancy for small path hop counts.

BIBLIOGRAPHY

[1] C. Bettstetter and C. Wagner, "The spatial node distribution of the random waypoint mobility model," in Proceedings of German Workshop on Mobile Ad Hoc Networks (WMAN), Ulm (Germany), March 2002.

[2] J. Chang and L. Tassiulas, "Energy Conserving Routing in Wireless Ad-hoc Networks," in Proceedings of IEEE Infocom, March 2000.

[3] D. B. Johnson, and D. A. Maltz, "Dynamic source routing in ad hoc wireless networks," *Mobile Computing*, pp. 153-181, 1996.

[4] C. Perkins and P. Bhagwat, "Highly dynamic destination-sequenced distance-vector routing (DSDV) for mobile computers," *Computer Communications Review*, Vol. 24(4), pp. 234-244, October 1994.

[5] C. Perkins and E. M. Royer, "Ad hoc on-demand distance vector routing," in Proceedings of the second annual IEEE workshop on mobile computing systems and applications, pp. 90-100, February 1999.

[6] V. Park and M. Corson, "A highly adaptive distributed routing algorithm for mobile wireless networks," in Proceedings of IEEE INFOCOM, April 1997.

[7] S. Murthy and J. J. Garcia-Luna-Aceves, "A Routing Protocol for Packet Radio Networks," in Proceedings of ACM First International Conference on Mobile Computing & Networking (MOBICOM'95), November, 1995.

[8] J. Raju and J. J. Garcia-Luna-Aceves, "A Comparison of On-demand and Table-driven Routing for Ad Hoc Wireless Networks," in Proceedings of IEEE ICC, June 2000.

[9] C.-C. Chiang, H.-k. Wu, W. Liu, and M. Gerla, "Routing in Clustered Multihop Mobile Wireless Networks with Fading Channel," in Proceedings of IEEE Singapore International Conference on Networks, 1997.

[10] Z. Haas and M. Peralman, "The Zone Routing Protocol (ZRP) for Ad Hoc Networks," in IETF MANET Draft, March, 2000.

[11] R. Dube, et al, "Signal Stability based Adaptive Routing (SSA) for Ad Hoc Mobile Networks," in IEEE Personal Communication Magazine, February, 1997.

[12] S. Singh, M. Woo and C. S. Raghavendra, "Power-Aware Routing in Mobile Ad Hoc Networks," in Proceedings of ACM/IEEE MOBICOM '98, October, 1998.

[13] P. Johansson, T. Larsson and N. Hedman, "Scenario-based Performance Analysis of Routing Protocols for Mobile Ad-hoc Networks," in Proceedings of IEEE/ACM/MOBICOM '99, pp. 195-206, August 1999.

[14] T. L. Fine, *Probability and Probabilistic Reasoning for Electrical Engineering*, Pearson Prentice Hall, Upper Saddle River (NJ), 2005.

[15] J. Galambos, *The Asymptotic Theory of Extreme Order Statistics*, John Wiley & Sons, New York (NY), 1978.

[16] P. Gupta and P. R. Kumar, "The capacity of wireless networks," *IEEE Transactions on Information Theory* **IT-46** (2000), pp. 388-404.

[17] Y. Han, R. J. La, and A. M. Makowski, "Distribution of path durations in mobile ad-hoc networks – Palm's Theorem at work," in Proceedings of the ITC Specialist Seminar on Performance Evaluation of Wireless and Mobile Systems, Antwerp (Belgium), August 2004.

[18] Y. Han and R. J. La, A. M. Makowski, and S. Lee, "Distribution of path durations in mobile ad-hoc networks – Palm's Theorem to the rescue," *to appear in Computer Networks (Special Issue on Network Modeling and Simulations, edited by P. R. Kumar and J. Hou).*

[19] Y. Han, "Distribution of path duration in wireless ad-hoc networks and its impact on rotuing," Doctoral Research Proposal, University of Maryland, College Park, April, 2005.

[20] Y. Han, R. J. La, and H. Zhang, "Path Selection in Mobile Ad-hoc Networks and Distribution of Path Duration," accepted to IEEE INFOCOM 2006.

[21] D. P. Heyman and M. J. Sobel, Stochastic Models in Operations Research, Volume I, McGraw-Hill, New York, New York, 1982.

[22] M. R. Leadbetter, "On extreme values in stationary sequences," Z. Wahrscheinlichkeitstheorie verw. Gebiete*, Vol. 28, pp. 289-303, 1974.*

[23] M. R. Leadbetter, "Extremes and local dependence in stationary sequences," Z. Wahrscheinlichkeitstheorie verw. Gebiete*, Vol. 65, pp. 291-306, 1983.*

[24] K. Fall and K. Varadhan, The ns Manual (formerly ns Notes and Documentation, The VINT project, UC Berkeley, LBL, USC/ISI, and Xerox PARC, November 1997. Available from http://www.isi.edu/nsnam/ns/doc/.

[25] IEEE, "Wireless LAN Medium Access Control (MAC) and Physical Layer (PHY) Specificationa," IEEE Std. 802.11-1997, 1997.

[26] T. Camp, J. Boleng, and V. Davies, "A Survey of Mobility Models for Ad Hoc Network Research," Wireless Communication and Mobile Computing (WCMC): Special

issue on Mobile Ad Hoc Networking: Research, Trends and Applications, vol. 2, no. 5, pp. 483-502, 2002.

[27] W. Navidi and T. Camp, "Stationary Distributions for the Random Waypoint Mobility Model," IEEE Transactions on Mobile Computing **ITMMC-3** *(2004), pp. 99-108.*

[28] J. Broch, D.A. Maltz, D. B. Johnson, Y.-C. Hu, and J. Jetcheva, "A performance comparison of multi-hop wireless ad hoc network routing protocols," in Mobile Computing and Networking(MobiCom), 1998, pp. 85-97.

[29] J. Yoon, M. Liu, and B. Noble, "Random Waypoint Considered Harmful," in Proc. 21st Ann. Joint Conf. IEEE Computer and Comm. Soc. (INFOCOM 2003), pp. 1312-1321, April, 2003.

[30] J. Yoon, M. Liu, and B. Noble, "Sound Mobility Models," in Proc. ACM/IEEE Int'l Conf. Mobile Computing and Networking (MOBICOM '03), pp. 205-216, September 2003.

[31] C. E. Perkins, Ad-hoc Networking, Addison-Wesley Longman, Incorporated, 2000.

[32] S. Ramanathan and E. Lloyd, "Scheduling Algorithms for Multi-hop Radio Networks," IEEE/ACM Transactions on Networking, Vol. 1(2), pp. 166-177, April 1993.

[33] V. Rodoplu and T. Meng "Minimum Energy Mobile Wireless Networks," IEEE Journal on Selected Areas in Communications, Vol. 17(8), pp. 1333-1344, August 1999.

[34] X. Hong, M. Gerla, G. Pei, and C.-C. Chiang, "A group mobility model for ad hoc wireless networks," in ACM/IEEE MSWiM, August, 1999.

[35] F. Bai and A. Helmy, "A Survey of Mobility Modeling and Analysis in Wireless Adhoc Networks," Book Chapter in submission to Kluwer Academic Publishers.

[36] *F. Bai, N. Sadagopan, and A. Helmy, "IMPORTANT: A framework to systematically analyze the Impact of Mobility on Performance of RouTing protocols for Adhoc NeTworks," in IEEE INFOCOM'03, San Francisco, March/April, 2003.*

[37] *N. Sadagopan, F. Bai, B. Krishnamachari, and A. Helmy, "PATHS: Analysis of path Duration statistics and the impact on reactive MANET routing protocols," in Proceedings of ACM MobiHoc, Annapolis (MD), June, 2003.*

[38] *C.-K. Toh, Ad-hoc Mobile Wireless Networks: Protocols and Systems, Prentice Hall PTR, 2001.*

[39] *C.-K. Toh, "A novel distributed routing protocol to support Ad hoc mobile computing," in Proceedings of IEEE 15th Annual Int'l. Conf. Comp. and Commun., pp. 480-486, March 1996.*

[40] *N. Maltz, J. Broch, J. Jetcheva, and D. Johnson, "The Effects of On-Demand Behavior in Routing Protocols for Multihop Wireless Ad Hoc Networks," in IEEE Journal on Selected Areas in Communications, Vol. 17, No. 8, Aug, 1999.*

[41] *G. S. Watson, "Extreme values in samples from m-dependent stationary processes,"* Ann. Math. Statist. *Vol. 25, pp. 798-800, 1954.*

[42] *R. D. Yates and D. J. Goodman, Probability and Stochastic Processes, Wiley, 1999.*